

Selection of Property Methods and Estimation of Physical Properties for Polymer Process Modeling

Y.A. Liu and Niket Sharma

Department of Chemical Engineering, Virginia Polytechnic Institute and State University,
Blacksburg, Virginia 24061, U.S.A.

Abstract

This chapter introduces novel methodologies for characterizing phase equilibrium and estimating physical properties crucial to polyolefin manufacturing. It presents an in-depth discussion on the polymer nonrandom two-liquid (POLYNRTL) activity coefficient model (ACM), and the polymer Sanchez-Lacombe (POLYSL) and the polymer perturbed-chain statistical fluid theory (POLYPCSF) equations of state (EOS). These innovative approaches offer specific guidelines for selecting the appropriate polymer ACM or EOS tailored to specific polyolefin processes.

A significant highlight is the detailed coverage of the POLYNRTL ACM, including a practical workshop for estimating POLYNRTL binary interaction parameters using the UNIFAC method. The chapter also explores the prediction of polymer physical properties through the Van Krevelen group contribution method, providing a hands-on workshop for estimating the physical properties of copolymers. Additionally, it introduces advanced techniques for parameter estimation using data regression tools, applied to both the POLYSL and POLYPCSF EOS models.

Furthermore, the chapter addresses the correlation of critical polyolefin product quality indices, such as melt flow rate or melt index and polymer density, providing insights that enhance the understanding and optimization of polyolefin manufacturing processes.

This is a preprint version of a chapter from our book - *Integrated Process Modeling, Advanced Control and Data Analytics for Optimizing Polyolefin Manufacturing*. Please cite the original work if referenced [52,56]

2.1 Property Methods and Thermophysical Parameter Requirements for Process Simulation

We present specific guidelines for the selection of an appropriate polymer ACM or EOS for modeling a specific polyolefin process [1,2].

This chapter begins by discussing the property methods and parameter requirements in simulating a polymer process (Section 2.1). We then present the polymer activity coefficient model (ACM), particularly the polymer non-random two-liquid (POLYNRTL) ACM in Section 2.2 and cover a workshop for estimating POLYNRTL binary interaction parameters using UNIFAC in Section 2.3. We discuss the prediction of polymer physical properties using the Van Krevelen group contribution method in Section 2.4. and follow by a workshop to estimate physical properties of a copolymer in Section 2.5. In Section 2.6, we introduce the polymer Sanchez-Lacombe (POLYSL) equation of state (EOS). Section 2.7 presents a workshop to estimate property parameters using data regression tool. Section 2.8 introduces the polymer perturbed-chain statistical fluid theory (POLYPCSF) EOS, and Section 2.9 presents a workshop for regression of property parameters for POLYPCSF EOS. In Section 2.10, we conclude this chapter by discussing the correlation of polyolefin product quality indices, such as melt flow rate or melt index and polymer density. Section 2.11 presents the bibliography.

Aspen Plus refers to a *property method* as a collection of models and methods for calculating phase equilibria and various physical properties, such as density, enthalpy, viscosity, thermal conductivity, etc. We will discuss two major categories of property methods, namely, the activity coefficient models (ACM) and equations of state (EOS), in the following sections, and provide guidelines on how to choose an appropriate property method for a specific polyolefin process.

Table 2.1 summarizes the key process modeling tasks and the essential thermophysical properties required for completing the tasks. The reader may search the information within Aspen Plus: Help -> Property requirements -> Property requirements for mass and energy balance simulations.

Table 2.1 Process modeling tasks and essential thermophysical property requirements

Process modeling task	Essential thermophysical property requirements
Mass balance	Density or standard liquid volume, phase equilibrium
Energy balance	heat capacity, heat of formation, heat of reaction, heat of vaporization, liquid vapor pressure
Heat transfer	Density, heat capacity, thermal conductivity, viscosity
Pressure drop	Density, viscosity

We discuss below the two key types of property methods for characterizing the phase equilibrium and estimating physical properties in polyolefin processes: activity coefficient model (ACM), and equation of state (EOS).

2.2 Polymer Activity Coefficient Models (ACM): Polymer Non-Random Two-Liquid (POLYNRTL) Model

In Chapter 6, we present the modeling of manufacturing processes for polystyrene (PS) using free radical polymerization, and for poly(styrene-butadiene-styrene) rubber or SBS rubber using ionic polymerization. For both processes, we must account for vapor-liquid equilibrium with a high degree of nonideality in the presence of polar components (such as water) at low to medium pressure (< 10 bar), that is away from the critical region [1,2]. In the discussion below, we follow the explanation in [3 to 5].

2.2.1 Vapor-Liquid Equilibrium for an Ideal Vapor Phase and a Nonideal Liquid Phase

Figure 2.1 shows a vapor-liquid mixture. We assume that the vapor phase is ideal. The partial pressure of component i in the vapor phase, P_i , is equal to:

$$P_i = x_i \gamma_i(x_i, T) P_i^{sat}(T) = y_i P \quad (2.1)$$

In the equation, x_i is the liquid mole fraction of component i , $\gamma_i(x_i, T)$ is the activity coefficient of component i as a function of liquid composition x_i and temperature T , $P_i^{sat}(T)$ is the vapor pressure of pure component i , y_i is the vapor mole fraction of component i , and P is the pressure.

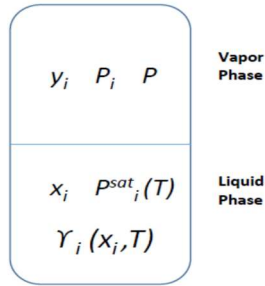


Figure 2.1 A vapor-liquid mixture.

For ideal solutions, the partial pressure P_i is equal to $x_i P_i^{sat}(T)$ according to Raoult's law [1]. For nonideal solutions, we correct this term by multiplying it with an activity coefficient, $\gamma_i(x_i, T)$. For an ideal vapor phase, the partial pressure P_i is equal to $y_i P$ according to Dalton's law [1].

2.2.2 General Vapor-Liquid Equilibrium Relationships Based on Fugacity Coefficient and Liquid-Phase Activity Coefficient

Based on Walas [1], we generalize Eq. (2.1) to define the vapor-liquid equilibrium using a gas-phase fugacity coefficient and a liquid-phase activity coefficient:

$$x_i \gamma_i f_i^{oL} = y_i \phi_i^V P = P_i \quad (2.2)$$

In the equation, f_i^{oL} is the liquid-phase reference fugacity, defined as the fugacity of a pure liquid at the temperature T and pressure P of the mixture, and ϕ_i^V is the partial gas-phase fugacity coefficient of component i computed from an equation of state.

2.2.3 Segment-Based Mole Fraction versus Species-Based Mole Fraction

This section follows the discussion in [3]. There are two types of molecular accounting systems that we use to model physical properties and phase equilibrium in polymer-containing systems. Species-based calculations consider polymer chains as single molecules, while segment-based accounting considers every polymer repeat unit ("segment") as an individual molecule. The segment-based approach can characterize polymer molecules by chemical properties of segments or monomer units that comprise the polymers. This makes it easier to evaluate the effect of polymer composition on thermodynamic properties. The segment-based approach can also consider the chain length, which is important in the modeling of phase equilibrium and physical properties.

Figure 2.2 illustrates a segment-based representation of polymer chains in a mixture, which permits the consideration of the interaction between each segment type and solvent molecules.

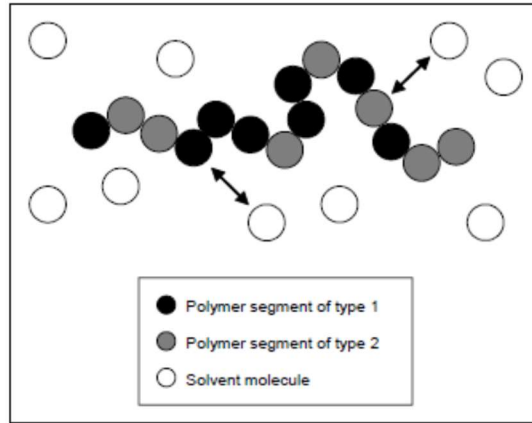


Figure 2.2 A segment-based representation of polymer chains in a mixture.

We note that the mole fraction of polymer chains is often of little physical significance. Let us consider a mixture of 1 g high-density polyethylene (HDPE) of a molecular weight 50,000, dissolved in 10 g of n-hexane of molecular weight 86.18. We find the mole fraction of polymer as:

$$X_{\text{polymer}} = (\text{moles polymer})/(\text{moles solvent} + \text{moles polymer}) = (1/50,000)/[1/86.18 + 1/50,000] = 1.72\text{E-}4$$

Now let us consider the ethylene segment (-C₂H₄-) of a molecular weight of 28.05. A HDPE polymer of a molecular weight of 50,000 corresponds to a degree of polymerization of 50,000/28.05, or 1534.9 segments. We treat each solvent molecule as a single segment. The segment-based mole fraction of polymer is then:

$$\begin{aligned} X_{\text{polymer}} &= (\text{moles polymer segments})/(\text{moles solvent} + \text{moles polymer segments}) \\ &= [(1/50,000) \times 1534.9] / [10/28.05 + (1/50,000) \times 1534.9] \\ &= 7.93\text{E-}2 \end{aligned}$$

This segment-based mole fraction is more representative of the amount of polymer in the mixture than the species-based mole fraction of polymer.

In general, we can convert the species-based mole fraction x to a segment-based mole fraction X according to the relationship [5]:

$$X_I = \frac{x_i r_{i,I}}{\sum_i \sum_I x_i r_{i,I}} \quad (2.3)$$

where subscript I refers to polymer segments, subscript i refers to a polymer molecule, and $r_{i,I}$ is the number of segment type I in polymer molecule i .

2.2.4 POLYNRTL: Polymer Nonrandom Two-Liquid Activity Coefficient Model

In the POLYNRTL model of Chen [4], the Gibbs free energy of mixing of a polymer solution is the sum of (1) the enthalpy of mixing, based on the nonrandom two-liquid (NRTL) theory [5], and (2) the entropy of mixing, based on the Flory-Huggins (F-H) theory [6 to 8]. The model calculates the activity coefficient as a sum of two contributions:

$$\ln \gamma_i = \ln \gamma_i^{NRTL} + \ln \gamma_i^{F-H} \quad (2.4)$$

where γ_i is the activity coefficient of species i , superscripts $NRTL$ and $F-H$ represents the NRTL and Flory-Huggins contributions, respectively.

We note that POLYNRTL and many other activity coefficient models ignore a third term in Eq. (2.3), representing the free-volume (FV) or compressibility contribution. Oishi and Prausnitz [9] proposed a UNIFAC-FV model to include the FV contribution. Interested readers may search “UNIFAC free volume model” in Aspen Plus online help to learn more detail about the model, but we do not use the model in this text.

The NRTL activity coefficient contribution is different for polymers (subscript $i=p$) and for solvents (subscript $i=s$). The relevant expressions are as follows.

$$\ln \gamma_{i=p}^{NRTL} = \sum_J \nu_{p,J} \left[\frac{\sum_K X_K G_{KJ} \tau_{KJ}}{\sum_K X_K G_{KJ}} + \sum_K \frac{X_K G_{JK}}{\sum_L X_L G_{LK}} \left(\tau_{JK} - \frac{\sum_L X_L G_{LK} \tau_{LK}}{\sum_L X_L G_{LK}} \right) \right] \quad (2.5)$$

$$\ln \gamma_{i=s}^{NRTL} = \frac{\sum_K X_K G_{Ks} \tau_{Ks}}{\sum_K X_K G_{Ks}} + \sum_L \frac{X_L G_{sL}}{\sum_K X_K G_{KL}} \left(\tau_{sL} - \frac{\sum_K X_K G_{KL} \tau_{KL}}{\sum_K X_K G_{KL}} \right) \quad (2.6)$$

In the equations, X_K is the segment-based mole fraction defined by Eq. (2.3). The parameter G_{ij} relates the overall segment-based mole fractions to the local segment-based mole fractions. It is related to the binary interaction parameter τ_{ij} and the nonrandomness factor α_{ij} through the following relationship:

$$G_{ij} = \exp(-\alpha_{ij} \tau_{ij}) \quad (2.7)$$

α_{ij} has a value between 0.2 to 0.3, and its value has no significant impact on the behavior of the model [5]. The binary interaction parameter τ_{ij} is related to the energy of interaction between species i and j , g_{ij} , and the energy of interaction between a pair of j species, g_{jj} , according to:

$$\tau_{ij} = (g_{ij} - g_{jj})/RT \quad (2.8)$$

This definition suggests that τ_{ii} is zero.

Aspen Plus databanks provide temperature-dependent relationships for both the binary interaction parameters τ_{ij} and the nonrandomness factor α_{ij} :

$$\tau_{ij} = a_{ij} + b_{ij}/T + e_{ij} \ln T + f_{ij} T \quad (2.9)$$

$$\alpha_{ij} = c_{ij} + d_{ij} (T - 273.15) \quad (2.10)$$

The Flory-Huggins contribution in Eq. (2.4) is as follows:

$$\ln \gamma_I^{FH} = \ln \left(\frac{\phi_I}{X_I} \right) + 1 - m_I \sum_J \left(\frac{\phi_J}{m_J} \right) \quad (2.11)$$

For a solvent, $\phi_i = X_i$, which is the segment-based mole fraction of the solvent; for a polymer, $\phi_i = X_i$, summed over all the segments.

m_i is the characteristic size of species i . It is related to the degree of polymerization by:

$$m_i = s_i \times P_i^{\varepsilon_i} \quad (2.12)$$

where s_i and ε_i are empirical parameters with default values for both being 1.0 for small molecules. P_i is the degree of polymerization of species i .

Table 2.2 summarizes the POLYNRTL model parameters. In using the POLYNRTL model within Aspen Plus/Polymers, we only need to enter parameters NRTL/1 to NRTL/8; Aspen Polymers sets the remaining model parameters to their default values.

Table 2.2 POLYNRTL model parameters

Parameter Name/Element	Symbol	Default	Unit Keyword	Comments
NRTL/1	a_{ij} and a_{ji}	0	---	Binary, Asymmetric
NRTL/2	b_{ij} and b_{ji}	0	TEMP	Binary, Asymmetric
NRTL/3	c_{ij}	0.3	---	Binary, Symmetric
NRTL/4	d_{ij}	0	1/TEMP	Binary, Symmetric
NRTL/5	e_{ij} and e_{ji}	0		Binary, Asymmetric
NRTL/6	f_{ij} and f_{ji}	0	1/TEMP	Binary, Asymmetric
NRTL/7	Tmin	0	TEMP	Unary
NRTL/8	Tmax	1000	TEMP	Unary
FHSIZE/1	s_i	1.0	---	Unary
FHSIZE/2	ε_i	1.0	---	Unary
POLDP	P_i	1.0	---	Unary

2.2.5 Concept of Henry Components for Vapor-Liquid Equilibrium for a Vapor Phase and a Nonideal Liquid Phase Involving Supercritical Components

A serious weakness of activity coefficient models is that they are not accurate in predicting the solubilities of supercritical components in the liquid phase. Those components refer to light gases and low molecular-weight hydrocarbons, such as H₂, O₂, N₂, CO, CO₂, H₂S, NO₂, SO₂, CH₄, C₂H₄, C₂H₆, C₃H₆, C₃H₈, etc. Refer to Eq. (2.1) for the vapor-liquid equilibrium relationship between an ideal vapor phase and a nonideal liquid phase:

$$P_i = x_i \gamma_i(x_i, T) P_i^{sat}(T) = y_i P \quad (2.1)$$

For a vapor phase and a nonideal liquid phase involving supercritical components, we modify Eq. (2.1) as:

$$x_i \gamma_i^* H_i = \phi_i^v y_i P = P_i \quad (2.13)$$

In the equation, $\gamma_i^* = Y_i / Y_\infty$, and Y_∞ is the infinite-dilution activity coefficient. H_i is the Henry's law constant, and ϕ_i^v is the vapor-phase fugacity coefficient calculated by an equation of state (EOS). For an ideal vapor phase, we choose the ideal gas law as the EOS; for a nonideal gas (such as a gas phase up to medium pressures), we use the Redlich-Kwong-Soave (RKS) EOS, which is a cubic EOS where the product of the pressure P and the third power (cubic) of the volume of the mixture, V_m^3 , is related to the ideal gas law constant R multiplied by the temperature T of the mixture. Interested reader may search "Redlich-Kwong-Soave" on Aspen Plus online help for details of the RKS EOS.

The Henry's law constant H_i is typically correlated as a function of temperature. For a supercritical component i and a solvent A , Aspen Plus uses the following correlation:

$$\ln(H_{i,A}) = a_{i,A} + b_{i,A}/T + c_{i,A} \ln T + d_{i,A} T + e_{i,A}/T^2 \quad T_L < T < T_H \quad (2.14)$$

Table 2.3 summarizes the Henry's law parameters.

Table 2.3 Henry's law parameters

Parameter Name/Element	Symbol	Default	Unit
Henry/1	$a_{i,A}$	0	---
Henry/2	$b_{i,A}$	0	TEMP
Henry/3	$c_{i,A}$	0	TEMP
Henry/4	$d_{i,A}$	0	TEMP
Henry/5	T_L	0	TEMP
Henry/6	T_H	2000	TEMP
Henry/7	$e_{i,A}$	0	TEMP

We demonstrate below how to implement the concept of Henry components and compare the resulting concentrations of light gases in the solvent *with and without* applying Henry's law. Consider a simple two-phase flash problem shown in Figure 2.3 and defined in Table 2.4. We save the simulation file as **Example 2.1 NRTL Flash with Henry Component.bkp**

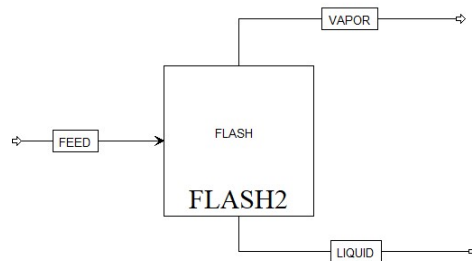


Figure 2.3 A simple flash unit for Example 2.1

Table 2.4 Specifications of Example 2.1

Components	Water, H2, N2
Property method	NRTL
Henry's components	H2, N2
Feed	70°C, 1 bar, Water (1000 kg/hr), H2(50 kg/hr), N2 (50 kg/hr)
Flash drum	70°C, 1 bar

Figure 2.4 illustrates how to specify Henry components: Properties -> Components -> Henry comps -> New: HC-1 -> Move H2 and N2 from “Available Components” to “Selected Component”.

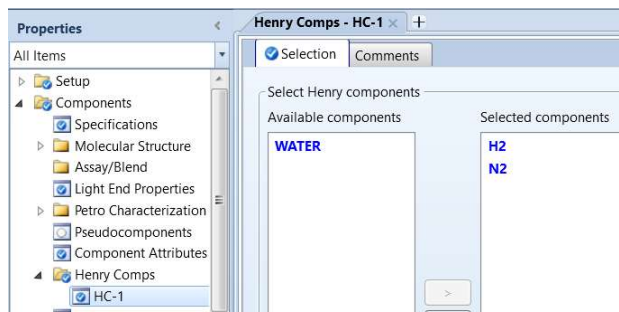


Figure 2.4 Specification of Henry's components, HC-1.

After defining the Henry components, we can see Henry's law parameters for both H2 and N2 by following the path: Properties -> Methods -> Parameters -> Binary Interaction -> HENRY-1 (see Figure 2.5). Refer to Eq. (2.13) and Table 2.3 for Henry parameters.

Component	Component	Source	Temperature units	Property units	AIJ	BIJ	CIJ	DIJ	TLOWE	TUPPER	EIJ
H2	WATER	APV110 BINARY	C	bar	180.066	-6993.51	-26.3119	0.0150431	0.85	65.85	0
N2	WATER	APV110 BINARY	C	bar	164.994	-8432.77	-21.558	-0.00843624	-0.15	72.85	0

Figure 2.5 Henry's law parameter values for H2-N2-water mixture.

Next, we enter the feed stream and flash conditions in Table 2.4. Subsequently, an inexperienced Aspen Plus user may follow the habit of clicking on the “Next” button and seeing a message of “required input complete” and proceed to run the simulation (see Figure 2.6).

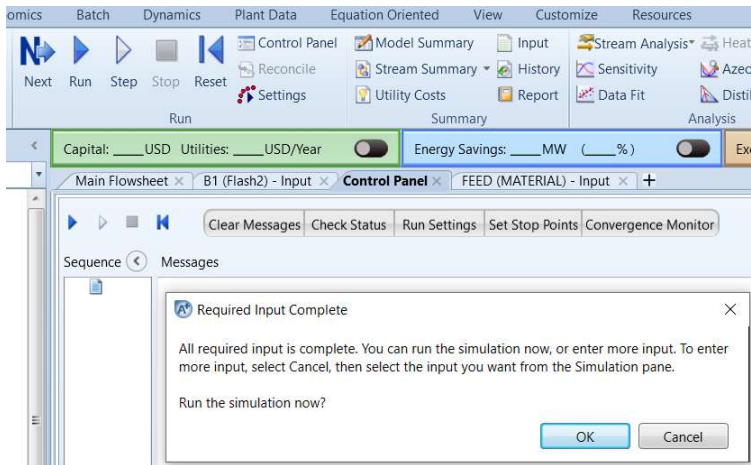


Figure 2.6 Clicking on the “Next” button, seeing the required input complete and clicking “OK” to run the simulation.

This results in the mass fractions of H₂ and N₂ in the LIQUID product being 4.98053E-6 and 5.25986E-5, or 4.98 and 52.5 ppm, respectively. See Figure 2.7. As we show shortly, despite having defined H₂ and N₂ as Henry components, these mass fractions actually result from the NRTL property method *without* incorporating the Henry’s law.

	Units	FEED	LIQUID	VAPOR
Molar Solid Fraction		0	0	0
Mass Vapor Fraction		0.288115	0	1
Mass Liquid Fraction		0.711885	1	0
Mass Solid Fraction		0	0	0
Molar Enthalpy	kcal/mol	-44.0272	-67.4398	-17.681
Mass Enthalpy	kcal/kg	-3285.88	-3743.56	-2155.04
Molar Entropy	cal/mol-K	-19.6117	-36.424	-0.692967
Mass Entropy	cal/gm-K	-1.46368	-2.02188	-0.0844617
Molar Density	kmol/cum	0.074436	52.6958	0.0350501
Mass Density	kg/cum	0.997359	949.31	0.287569
Enthalpy Flow	Gcal/hr	-3.61447	-2.93148	-0.682988
Average MW		13.3989	18.0149	8.20452
Mass Flows	kg/hr	1100	783.074	316.926
Mass Fractions				
WATER		0.909091	0.999942	0.684611
H ₂		0.0454545	4.98053e-06	0.157753
N ₂		0.0454545	5.25986e-05	0.157636

Figure 2.7 Computed mass fractions of H₂ and N₂ in the LIQUID product without incorporating Henry’s law into the NRTL property method

To incorporate Henry’s law into the calculation of the NRTL property method, we must tell Aspen Plus to do so following the path: Property -> Methods -> Specification -> Henry components -> HC-1 defined in Figure 2.3. We illustrate this step in Figure 2.8.

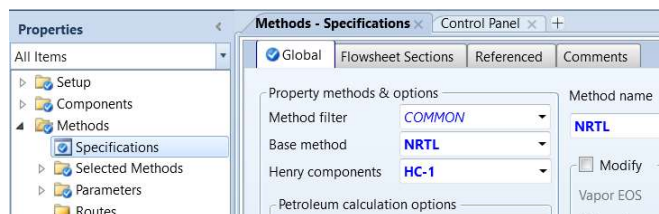


Figure 2.8 Including Henry components HC-1 into the NRTL property method.

Running the simulation again, we see in Figure 2.9 the resulting the mass fractions of H2 and N2 in the LIQUID product being 9.47979E-7 and 6.16813E-7, or 0.948 and 0.617 ppm, respectively (compared to the incorrect values of 4.98 and 52.5 ppm in Figure 2.7). The significant difference demonstrates the importance of correctly including Henry components into the NRTL property method. This observation applies to the POLYNRTL property method as well.

Flowsheet x Control Panel x B1 (Flash2) - Stream Results (Boundary) x +						
Material	Vol.% Curves	Wt. % Curves	Petroleum	Polymers	Solids	
			Units	FEED	LIQUID	VAPOR
Molar Solid Fraction				0	0	0
Mass Vapor Fraction				0.288197	0	1
Mass Liquid Fraction				0.711803	1	0
Mass Solid Fraction				0	0	0
Molar Enthalpy			kcal/mol	-44.0268	-67.4445	-17.6823
Mass Enthalpy			kcal/kg	-3285.86	-3743.77	-2154.89
Molar Entropy			cal/mol-K	-19.6109	-36.4269	-0.693001
Mass Entropy			cal/gm-K	-1.46362	-2.02202	-0.0844539
Molar Density			kmol/cum	0.0744252	52.7001	0.0350501
Mass Density			kg/cum	0.997215	949.401	0.287609
Enthalpy Flow			Gcal/hr	-3.61444	-2.93131	-0.683135
Average MW				13.3989	18.0151	8.20567
+ Mass Flows			kg/hr	1100	782.984	317.016
- Mass Fractions						
WATER				0.909091	0.999998	0.684563
H2				0.0454545	9.47979e-07	0.157718
N2				0.0454545	6.16813e-07	0.157719

Figure 2.9 Computed mass fractions of H2 and N2 in the LIQUID product after incorporating Henry's law into the NRTL property method.

To summarize, the POLYNRTL method is applicable to polyolefin processes involving a highly nonideal liquid phase (with polar and hydrogen-bonding species) up to medium pressures of approximately 10 bar. It must be used with Henry's law when the mixture contains light gases and low molecular-weight hydrocarbons. Two typical processes are polystyrene (PS) using free radical polymerization, and poly(styrene-butadiene-styrene) rubber or SBS rubber using ionic polymerization discussed in Chapter 6. For non-polyolefin systems, we apply the POLYNRTL method to Nylon, PET (polyethylene terephthalate), and PLA (polylactic acid), etc. for step-growth polymerization processes [3].

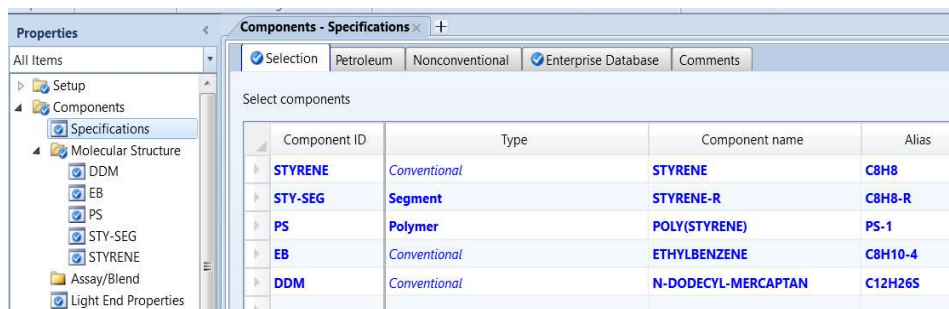
2.3 Workshop 2.1 Estimating POLYNRTL Binary Parameters Using UNIFAC

2.3.1 Objective:

The UNIFAC (UNIQUE Functional-group Activity Coefficients) method [10,11] is a semi-empirical system for the prediction of non-electrolyte activity in non-ideal mixtures. Over the years, there have been numerous articles and books extending the method to more complex vapor-liquid mixtures. The UNIFAC method attempts to break down the problem of predicting interactions between molecules by describing molecular interactions based upon functional groups, such as functional groups 1005 (>CH-), 1100 (>CH2), 1015 (-CH3), and 2400 (CH2SH), attached to the molecule. A search of Aspen Plus online help for "UNIFAC Functional Groups" will give Tables 3.12 to 3.21 of the functional groups available within Aspen Plus. This workshop demonstrates how to use UNIFAC to estimate POLYNRTL binary parameters.

2.3.2 Estimating POLYNRTL Binary Parameters Using UNIFAC for Polystyrene Manufacturing

Figure 2.10 shows some of the components involved in polystyrene manufacturing, where Sty and STY-SEG are styrene (monomer) and STY-SEG are styrene segment (repeat unit), and EB (ethyl benzene) and DDM (n-dodecyl mercaptain) are chain-transfer agents. We save the simulation file as **WS2.1 Estimating POLYNRTL Binary Parameters Using UNIFAC.bkp**.



Component ID	Type	Component name	Alias
STYRENE	Conventional	STYRENE	C8H8
STY-SEG	Segment	STYRENE-R	C8H8-R
PS	Polymer	POLY(STYRENE)	PS-1
EB	Conventional	ETHYLBENZENE	C8H10-4
DDM	Conventional	N-DODECYL-MERCAPTAN	C12H26S

Figure 2.10 Component specifications for WS 2.1.

If a component is present in the Aspen Enterprise Database for pure components and segments, we will see its structure being displayed within the “Molecular Structure” folder, as illustrated in Figure 2.11 for DDM (C₁₂H₂₆S). Additionally, Aspen Plus will automatically complete a representation of the displayed structure as a combination of UNIFAC functional groups, that is, C₁₂H₂₆S = H₃C-(CH₂)₁₀-CH₂SH = 1*(Group 1015, H₃C) + 10*(Group 1100, CH₂) + 1*(Group 2400, CH₂SH). In fact, Aspen Plus will do this for all specified components that are present in the Aspen Enterprise Database, which will enable the use of UNIFAC group-contribution method to estimate the binary parameters.

We see a “Draw/Import/Edit” button in Figure 2.11. In Section 4.4.3, we will show how to import a molecular structure file, *.mol, from the Internet (such as Chemical Book, www.chemicalbook.com) for a component not available within Aspen Enterprise Database. In Section 6.1.4, we also demonstrate how to use the drawing tools within Aspen Plus to draw a molecular structure.

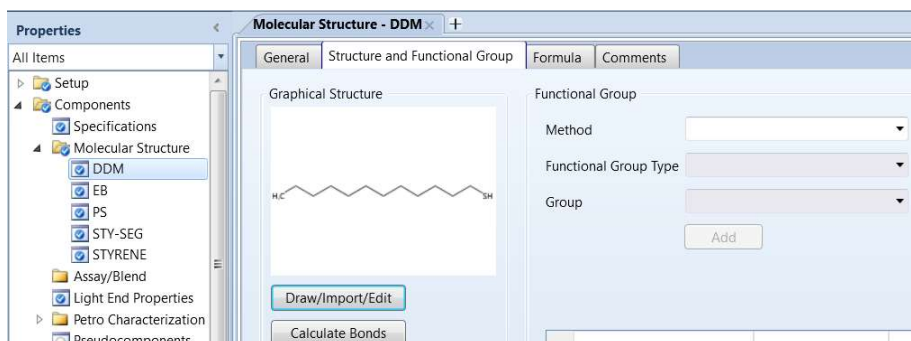


Figure 2.11 Showing a graphical structure of DDM (n-dodecyl-mercaptan) available in the Aspen Enterprise Database.

Next, we follow the path: Properties -> Estimation -> Input -> (1) Estimation Option -> Estimate only the selected parameters; (2) Parameter type -> Binary interaction parameters (see Figure 2.12).

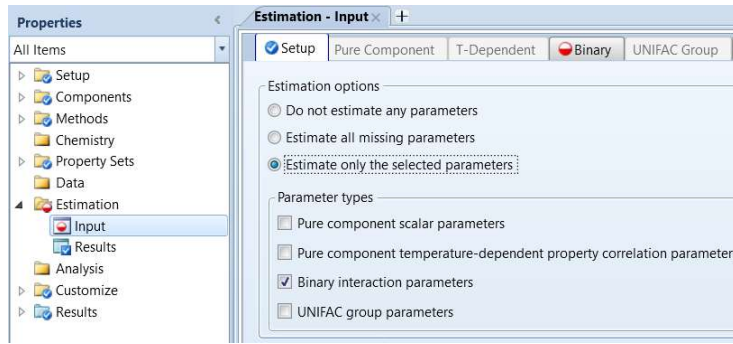


Figure 2.12 Specification to estimate binary interaction parameters.

In Figure 2.13, we click on the “New” button, and then choose parameter, “NRTL” and method “UNIFAC”. We can specify component i (STYRENE) and component j (STY-SEG) and other i - j component combination one by one. However, this is not necessary; by choosing “ALL” for both components i and j , Aspen Plus will estimate the interaction parameters for all binary component combinations for us.



Figure 2.13 Specification of binary interaction parameters to be estimated

We then run the property estimation. Figure 2.14 shows the estimated binary interaction parameters, according to Eqs. (2.9) and (2.10) and Table 2.2. We save the simulation file as **WS 2.1 Estimating Binary Parameters from UNIFAC.bkp**.

Component i	Component j	a_{ij}	a_{ji}	b_{ij}	b_{ji}	Alpha	Method
STYRENE	STY-SEG			65.8755	-50.1147	0.3	UNIFAC
STYRENE	EB			-134.461	147.181	0.3	UNIFAC
STYRENE	DDM			-121.084	87.1706	0.3	UNIFAC
STY-SEG	EB			105.46	-79.4476	0.3	UNIFAC
STY-SEG	DDM			391.35	-252.193	0.3	UNIFAC
EB	DDM			-176.542	205.584	0.3	UNIFAC

Figure 2.14 Estimated binary interaction parameters.

Additionally, by following the path, Properties -> Methods -> Parameters -> Binary Interaction -> NRTL-1, we also see the estimated parameters being entered as the result (R) of the Physical Constant Estimation System (PCES), that is, R-PCES. See Figure 2.15.

Component i	Component j	Source	Temperature units	AU	AJI	BIJ	BJI	CIJ	DIJ	EIJ	EJI	FIJ	FJI	TLOWER	TUPPER
STYRENE	EB	APV110 VLE-IG	C	-0.975	1.385	37.6404	-56.0044	0.3	0	0	0	0	0	57.67	97
STYRENE	STY-SEG	R-PCES	C	0	0	65.8755	-50.1147	0.3	0	0	0	0	0	25	25
STY-SEG	EB	R-PCES	C	0	0	105.46	-79.4476	0.3	0	0	0	0	0	25	25
STYRENE	DDM	R-PCES	C	0	0	-121.084	87.1706	0.3	0	0	0	0	0	25	25
STY-SEG	DDM	R-PCES	C	0	0	391.35	-252.193	0.3	0	0	0	0	0	25	25
EB	DDM	R-PCES	C	0	0	-176.542	205.584	0.3	0	0	0	0	0	25	25

Figure 2.15 Entering the estimated binary interaction parameters to the “parameters” form.

2.4 Prediction of Polymer Physical Properties by Van Krevelen Functional Group Method

As we discussed vapor-liquid equilibrium according to Eq. (2.12), the POLYNRTL property method uses the POLYNRTL activity coefficient model for the liquid phase and applies the RKS (Redlich-Kwong-Soave) [12] cubic equation of state for the vapor phase. For property calculations, *the POLYNRTL property method uses Van Krevelen functional group method to predict physical properties of polymers.*

The Van Krevelen method is based on the chemical structure of the polymers [13]. Table 2.5 summarizes the key concepts of applying the Van Krevelen method. A search of the online help of Aspen Plus for “Thermophysical Properties of Polymers” will show the large number of polymer properties that we can estimate by the Van Krevelen method.

Table 2.5 Applying the Van Krevelen method to estimate properties of a system containing polymers by going from functional groups to segments and then to polymer mixture

1. -CH2-	Functional group (Van Krevelen; VK)	Estimate segment properties using properties of the functional groups making up the segment(s), e.g., heat capacity C_p , $C_p = \sum_k n_k C_{p,k}$ k refers to k -th functional group; n_k is the number of the k -th functional group. When retrieving the segments from the SEGMENT databank, there is no need to supply functional groups. Otherwise, define the segments based on the VK functional groups.
2. -CH2-CH2-	Segment (ethylene)	Calculate polymer properties from segment properties, number-average degree of polymerization, and segment composition.

3. -CH ₂ -CH ₂ -CH ₂ -CH ₂ -....	Polymer (polyethylene)	Find the mixture properties of the whole component system (polymer, monomer, solvents, etc.).
---	------------------------	---

Let us illustrate the concept of the Van Krevelen method by considering the molar volume of a polymeric component, which depends on the temperature and the physical state of the polymer. Figure 2.16 shows a plot of the molar volume versus temperature of a polymer at different physical states. In the figure, V_l refers to the molar volume of a polymer liquid, V_c indicates the molar volume of a crystalline polymer, and V_g represents the molar volume of an amorphous glassy polymer. X_c represents the mass fraction of a crystalline polymer. T_g and T_m are, respectively, the glass transition temperature and the melting transition temperature. These volume and temperature concepts are well explained in most introductory polymer textbooks [e.g., 14].

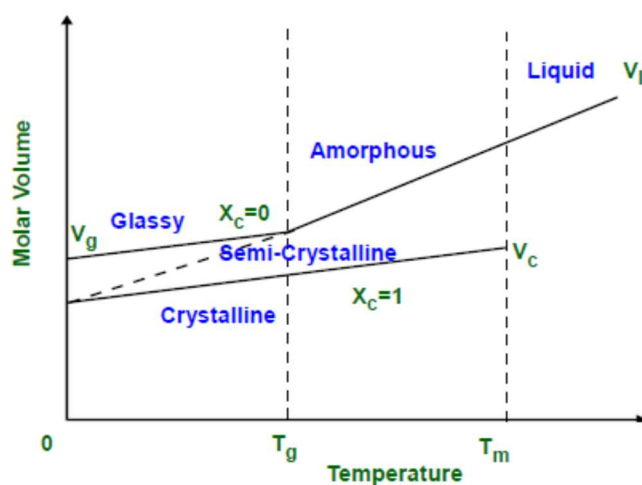


Figure 2.16 Molar volume versus temperature for different physical states of a polymer.

The basic idea of a group contribution method for estimating physical properties of polymers is to calculate the sum of contributions of the constituents (the structural and functional groups) as an approximation. Consider, for example, finding the molar density of a propylene repeat segment illustrated in Figure 2.17.

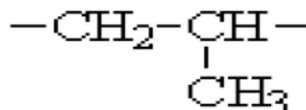


Figure 2.17 A propylene repeat segment C₃H₆-R.

The molecular weight of this structural unit is 42.08 g/mol. From Table 4.5 in Van Krevelen and Nijenhuis [13], we know the Van der Waals volume (V_w) contribution of Van Krevelen functional group 100, -CH₂-,

at 25°C is 16.1 cm³/mol, and that of group 101, -CH(CH₃)-, is 33.2 cm³/mol. The additive sum of both volume contributions is 49.3 cm³/mol. Therefore, the molar density of a propylene repeat segment at 25°C is: [42.08 g/mol]/[49.3 cm³/mol], or 0.85 g/cm³. This value is in perfect agreement with the experimental value [13]. We note, however, that not every property prediction by the Van Krevelen method matches perfectly with experimental data.

When we cannot neglect the interactions between functional and structural groups, the Van Krevelen method includes correction terms for the interactions. The resulting models are called *group interaction models* [13]. Interested readers can find additional details about the Van Krevelen method for estimating physical properties by searching Aspen Plus online help for “Van Krevelen group contribution methods”.

2.5 Workshop 2.2 Estimating Physical Properties of a Copolymer Using the Van Krevelen Group Contribution Method

2.5.1 Objective:

This workshop demonstrates the procedure of applying the Van Krevelen group contribution method to estimate physical properties of a copolymer. These properties include, for example, CP (heat capacity), K (thermal conductivity), MU (viscosity), RHO (density), TG (glass transition temperature) and TM (melting transition temperature). We use styrene-butadiene rubber (SBR) that we shall discuss in more detail in Chapter 6 as our copolymer, and assume the copolymer with a number-average degree of polymerization (DPN) of 2000. We study the flash operation of a SB copolymer consisting of 50% by mole styrene and 50% by mole butadiene at 250° and 1.01325 bar. We assume the mass flow rates of the styrene, butadiene and SB copolymer are identical, each at 10 kg/hr.

We show how to apply the Van Krevelen method according to the following steps: (1) drawing the process flowsheet; (2) specify the unit set and global options; (3) define components, segments and polymer, and characterize their structures; (4) choose property method and enter or estimate property parameters; (5) define streams and blocks; (6) create property sets; (7) define property analysis runs to create property tables; and (8) run the simulation, examining the results and make property plots.

2.5.2 Draw the Process Flowsheet, and Specify the Unit Set and Global Options

Our simple flash unit is the same as in Figure 2.3. We choose the unit set METCBAR in Setup in both Properties and Simulation, as demonstrated previously in Figure 1.7. For global options, we follow the path: Simulation -> Setup -> Global settings -> Flow basis: choose “Mass” (see Figure 1.6).

2.5.3 Define Components, Segments and Polymer, and Characterize Their Structures

Figure 2.18 shows our component specifications. We note two points: (1) We purposely do not specify the component name and alias (chemical formula) of the styrene segment, STY-SEG, as we want to demonstrate how to use Van Krevelen functional groups to specify this segment; and (2) We specify the styrene-butadiene copolymer with a number-average degree of polymerization, DPN, defined in Eqs. (1.5) and (1.11), of 2000, as a “generic polymer component” with an alias “polymer”.

Component ID	Type	Component name	Alias
STY-SEG	Segment		
STYRENE	Conventional	STYRENE	C8H8
BUT-SEG	Segment	BUTADIENE-R-1	C4H6-R-1
BUTADIEN	Conventional	1,3-BUTADIENE	C4H6-4
SB	Polymer	GENERIC-POLYMER-COMPONENT	POLYMER

Figure 2.18 Component specifications

To characterize the polymer component, we follow the path: Properties -> Components -> Polymer -> Segments -> Segment definition: Choose “Repeat” unit for both STY-SEG and BUT-SEG. Figure 2.19 shows our selection of the built-in polymer attributes for “Properties Selection” for our SB copolymer. See Figure 1.19. We have previously explained all the selected attributes in Sections 1.3.2 and 1.3.3.

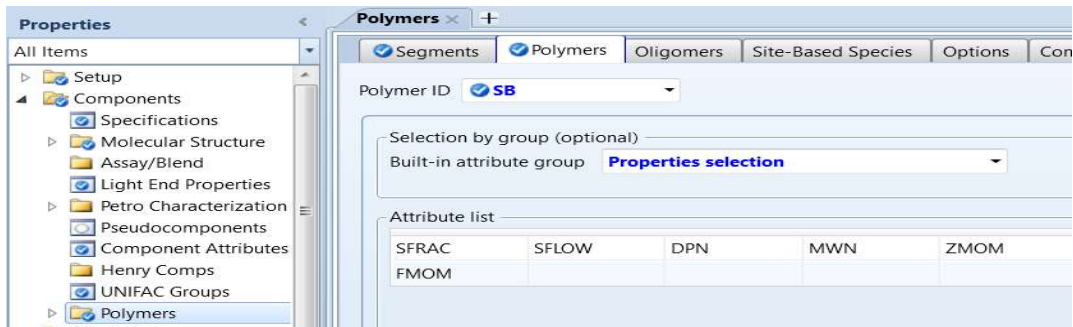


Figure 2.19 Choosing the built-in “Properties selection” attribute group.

Next, we check the path: Properties ->Components -> Molecular structure -> Structural and functional groups, and note that segment BUT-SEG, and pure components BUTADIEN and STYRENE are available within Aspen Plus segment and component databanks, and we see their structures being displayed. We do not need the structure of the generic polymer component, SB copolymer, but we need to specify the structure of the segment STY-SEG, as shown in Figure 2.20.

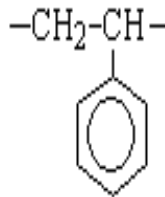


Figure 2.20 Structure of STY-SEGA

A search of Aspen Plus online help on “Van Krevelen Functional Group Parameters” shows that we can represent STY-SEG as a sum of three Van Krevelen (VK) functional groups: (1) VK group 100, -CH₂-; (2) VK group 131, >CH-; and (3) VK group 146, benzyl group. We specify these groups according to Figure 2.21.

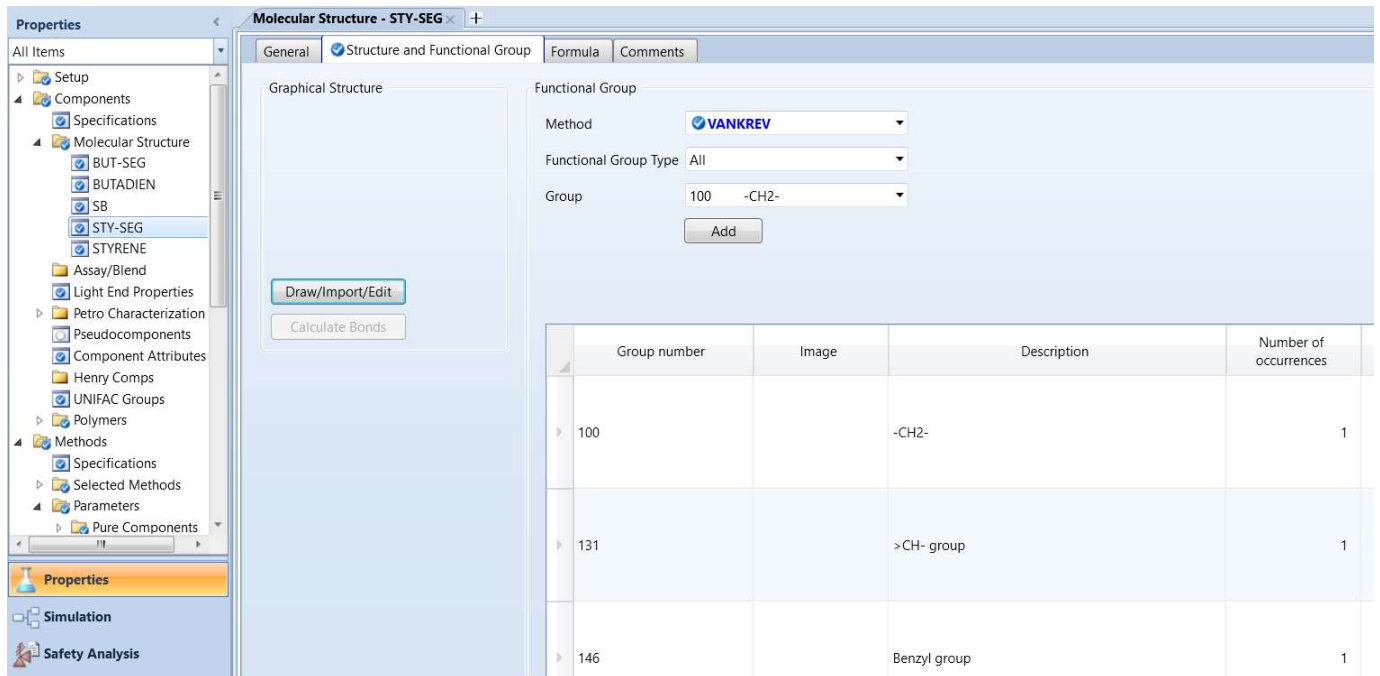


Figure 2.21 Specifications of Van Krevelen functional groups for STY-SEG

2.5.4 Choosing Property Method and Entering or Estimating Property Parameters

We choose the POLYNRTL property method for the current problem, as in our detailed styrene-butadiene rubber (SBR) workshop in Chapter 6. Following exactly Workshop 2.1, Section 2.6, we estimate all missing binary interaction parameters. Figure 2.22 shows the estimated binary parameters.

Component 1	Component 2	Source	Temperature units	A1J	A2J	B1J	B2J	C1J	C2J	TLOW	TUPPER	
STYRENE	BUT-SEG	R-PCES	C	0	0	-24.2903	17.9355	0.3	0	0	25	25
STYRENE	BUTADIEN	R-PCES	C	0	0	-131.901	223.243	0.3	0	0	25	25
BUT-SEG	BUTADIEN	R-PCES	C	0	0	-81.3649	133.427	0.3	0	0	25	25

Figure 2.22 Estimated binary interaction parameters

2.5.5 Specifications of Feed Stream and Flash Block

Figure 2.23 shows the specification of feed stream. Under component attributes, we need to specify the SFRAC, SFLOW and DPN for SB copolymer.

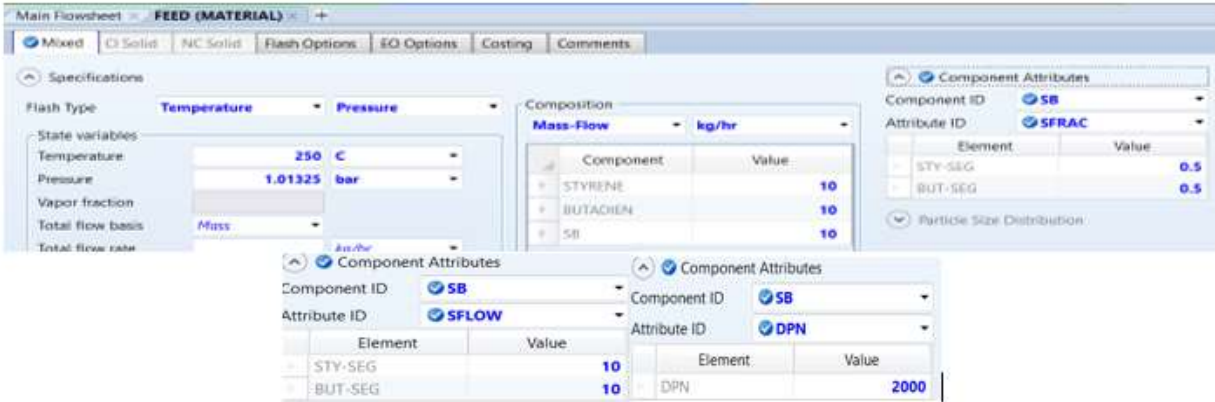


Figure 2.23 Specification of feed stream with component attributes SFRAC, SFLOW and DPN for the generic polymer component, SB copolymer.

For the flash unit, we enter a temperature of 250°C and a pressure of 1.01325 bar.

2.5.6 Creating Property Sets

A *property set* is a collection of thermodynamic, transport, and other properties that we can use in stream reports, physical property tables and analysis, heating and cooling curves of unit operation models (e.g., exchanger, condenser, and reboiler), distillation column stage property reports, reactor temperature profiles, etc.

We create a property set to display the property values that we find from a physical property analysis. We define a property set in either the Properties or Simulation environment, and the resulting property set will appear in both environments. We follow the path: Properties -> Property sets -> New; name- PS-1 -> Properties and Qualifiers (see Figures 2.24 and 2.25). Note the pull-down menu of physical properties and the corresponding units for the user to choose. We include *CP* (heat capacity), *K* (thermal conductivity), *MU* (viscosity), *RHO* (density), *TG* (glass transition temperature) and *TM* (melting transition temperature) in the property set.

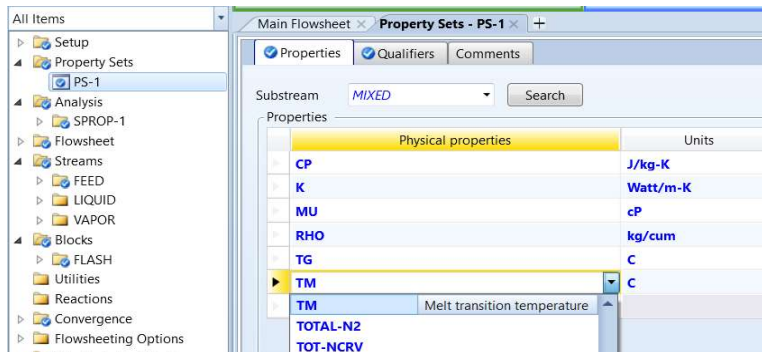


Figure 2.24 Including physical properties in the property set PS-1

Property	Value	Value	Value
Phase	Liquid		
Component	STYRENE	BUTADIEN	SB
2nd liquid key component			
Temperature	<input checked="" type="checkbox"/> System	C	
Pressure	<input checked="" type="checkbox"/> System	bar	
% Distilled			

Figure 2.25 Qualifiers for selected properties in the property set.

To ensure that the stream report from our flash unit includes values of the specified properties in the property set PS-1, we follow the path: Simulation -> Setup -> Report Options -> Streams -> Click on “Property Sets” button -> Property Sets: Move PS-1 from Available property sets to Selected property sets -> Close. See Figure 2.26.

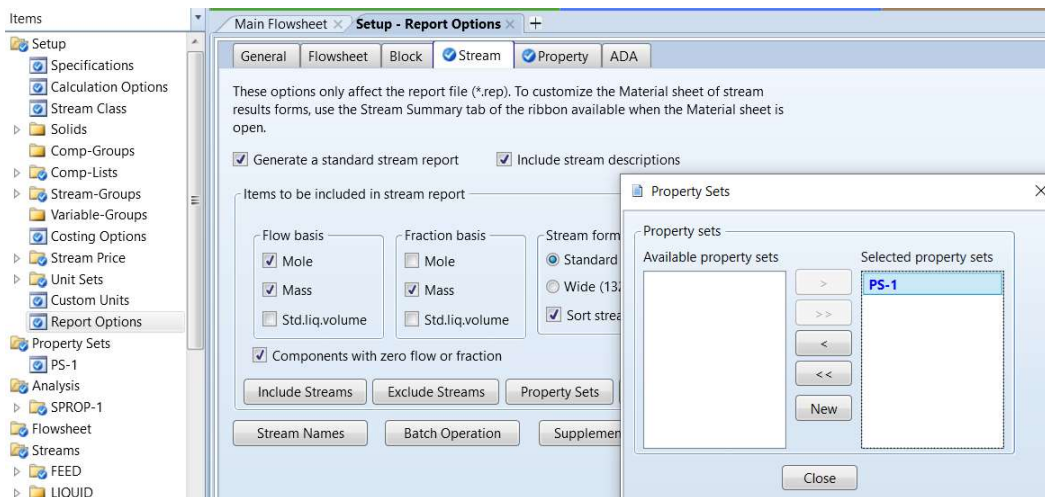


Figure 2.26 Including specified property set PS-1 in the stream report

2.5.7 Defining Property Analysis Run to Create Property Tables

We can use property analysis tool to generate tables and plots of physical properties of pure components and mixtures as a function of temperature, pressure, and composition. We should emphasize that both property analysis and regression tools in Aspen Plus do **not** support polymer attributes. Therefore, for property analysis and regression runs, we should define a polymer as an oligomer. By doing so, we eliminate the need to enter any attribute information. We should specify its number of repeat units or segments, and segment composition (following the path: Components -> Polymers -> Characterization -> Oligomers -> Oligomer Structure -> Fill in the number of repeat units), and degree of polymerization. Alternatively, as in the current example, we specify the SB copolymer as a *generic polymer component* with an alias “polymer”, and specify its attributes, particularly segment composition by SFRAC and its degree of polymerization (see Figure 2.18 and 2.23).

We create an analysis of stream properties by following the path: Process flowsheet -> Right-click the name of FEED steam -> Choose “Analysis” on the pull-down menu -> Choose analysis type, “Stream Properties”. See Figures 2.27 and 2.28. We then click on the “Run Analysis” button on Figure 2.28 to do stream property analysis. When the analysis is completed, we click on the “Results” button displayed in Figure 2.28 and follow the same approach as in Figures 1.22 and 1.23 to make a “custom” plot of

properties (CP, K, MU and RHO) versus temperature. Figures 2.29 and 2.30 illustrate the resulting plots of thermal conductivity and mass density versus temperature. The tabulated analysis results also show the glass transition temperature and the melt transition temperature of the SB copolymer are 45.3472°C and 225.23°C, respectively. This concludes the current workshop. We save the simulation file as **WS 2.2 Estimating Physical Properties of a Copolymer Using VK Group Contribution Method.bkp**.

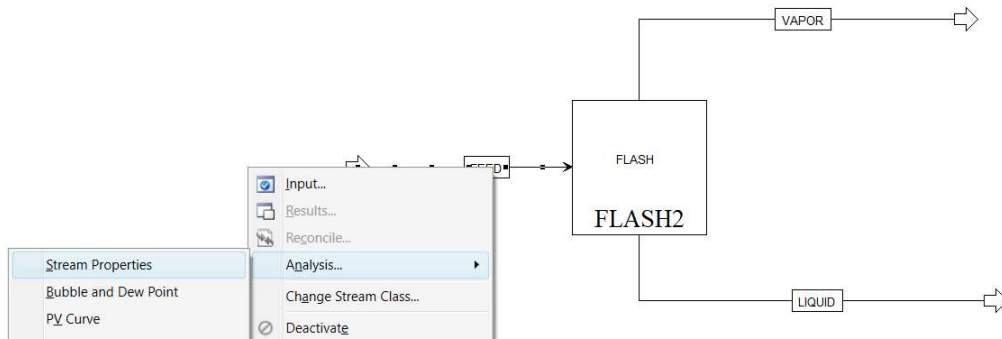


Figure 2.27 Initiating an analysis of stream properties for FEED stream

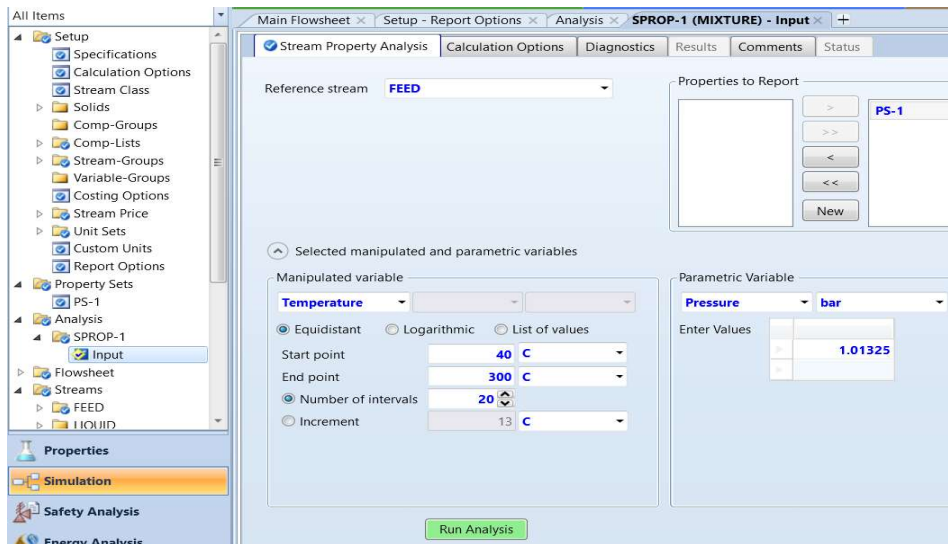


Figure 2.28 Specification of stream property analysis (SPROP-1)

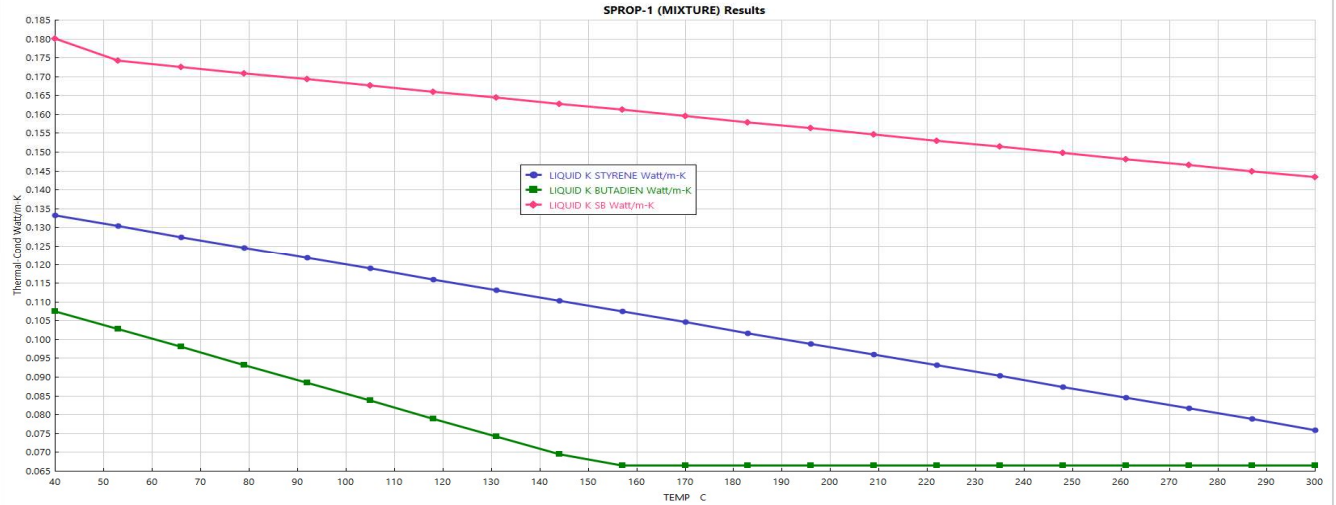


Figure 2.29. Thermal conductivity (K) of styrene, butadiene, and SB copolymer versus temperature.

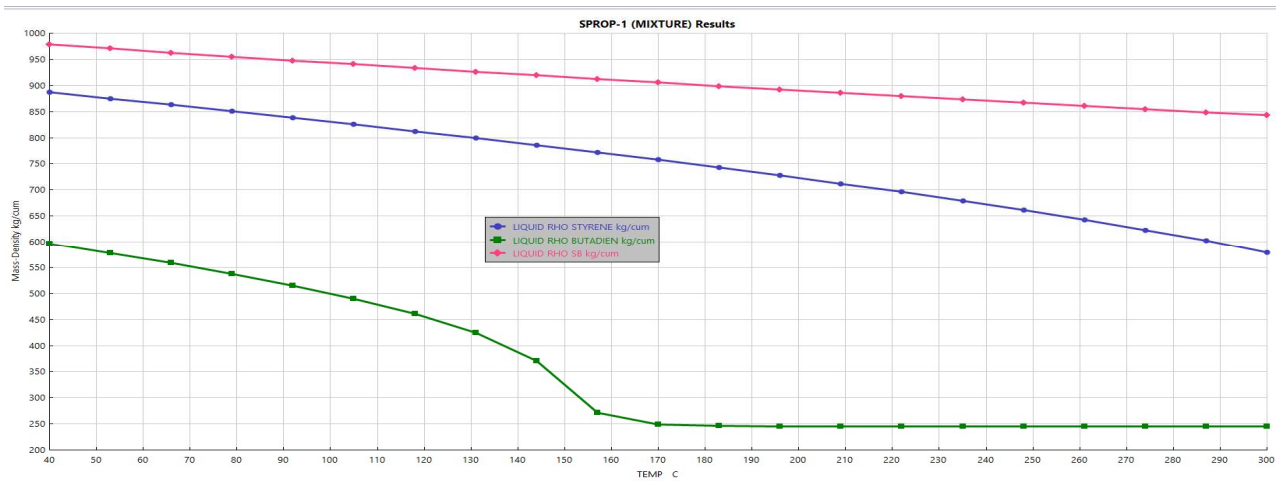


Figure 2.30 Mass density (RHO) of styrene, butadiene, and SB copolymer versus temperature.

2.6 Polymer Sanchez-Lacombe Equation of State (POLYSL)

To simulate polyolefin processes at high pressures, activity coefficient models, such as POLYNRTL, suffer from some weaknesses, as most of them are applicable only to incompressible liquid solutions. Additionally, activity coefficient models fail to predict correctly the phase behavior of polymer solutions at the lower critical solution temperature (LCST) below which the components of a mixture are miscible for all compositions. Activity coefficient models also fail to predict an upper bound to a temperature interval of partial miscibility, called the upper critical solution temperature (UCST). By contrast, an equation of state (EOS) can accurately represent the relationship among temperature, pressure, volume (or density) and composition of a vapor-liquid, or vapor-liquid-liquid mixture over the *entire* fluid region. *EOS models can evaluate the physical properties of any fluid phase, liquid and/or vapor at medium to high pressures, as long as the fluid mixture does not contain any polar components.* References [16,17] reviewed the development of EOSs for mixtures involving pure components, oligomers, and polymers.

Two of the most useful EOSs for modeling polyolefin processes are: (1) Polymer Sanchez-Lacombe (POLYSL) EOS [18 to 20]; and (2) polymer perturbed-chain, statistical fluid theory (POLYPCSF) EOS [21 to 23], an extension of the statistical fluid theory (SAFT) EOS [24 to 26]. We discuss the POLYSL EOS below.

The Sanchez-Lacombe EOS is known as a lattice-gas model since the P-V-T properties of a pure component are calculated *assuming the component is broken into parts or “mers” that are placed into a lattice and are allowed to interact with a mean-field-type intermolecular potential* [20]. The Sanchez-Lacombe EOS for pure fluids is:

$$\tilde{\rho}^2 + \tilde{P} + \tilde{T} \left[\ln(1 - \tilde{\rho}) + \left(1 - \frac{1}{m}\right) \tilde{\rho} \right] = 0 \quad (2.15)$$

where

$$\tilde{T} = \frac{T}{T^*} \quad \tilde{P} = \frac{P}{P^*} \quad \tilde{\rho} = \frac{\rho}{\rho^*} \quad (2.16)$$

with

$$T^* = \frac{\varepsilon^*}{k} \quad P^* = \frac{\varepsilon^*}{v^*} \quad \rho^* = \frac{M}{mv^*} \quad (2.17)$$

In these equations, T is absolute temperature (K), P is pressure (bar), ρ is density (kg/m³). \tilde{T} , \tilde{P} , and $\tilde{\rho}$ are the reduced temperature, pressure, and density, respectively. T^* (K), P^* (bar) and ρ^* (kg/m³) are scale factors that are independent of molecular size of the polymer. ε^* is a characteristic interaction energy per segment. k is the Boltzmann constant, which is a proportionality constant between the quantities temperature (with unit kelvin) and energy (with unit joule), with a value of 1.380649E-23 J/K. v^* is the closed-packed volume of a segment. M is the molecular weight, and m is the number of segments per chain.

We typically determine the scale factors, T^* (K), P^* (bar) and ρ^* (kg/m³), from regressing experimental data, such as vapor-pressure data for conventional components and liquid-volume data for polymer species. We will demonstrate how to do this in a workshop in the next section. A search of “Sanchez-Lacombe unary parameters” in Aspen Plus online help gives the values of these unary parameters for many polymers, solvents, and monomers; and several published articles also give the regressed unary parameters for selected segments in simulating HDPE, LDPE and LLDPE processes [28 to 31]. Figure 2.31 gives examples of POLYSL unary (or pure component) parameters for simulating a slurry HDPE copolymerization process [28]. In the figure, TICL4 and TEAL (triethyl aluminum) are catalyst and cocatalyst. CH4, C2H6 and N2 are impurities. C2H4 and C4H8 are monomer and comonomer. R-C2H4 and R-C4H8 are ethylene and 1-butene segments, and H2 is the chain transfer agent. To enter these parameter values, we follow the path: Properties -> Methods -> Parameters -> Pure Components -> New: name = PURE-1 -> Parameters: SLTSTR, SLPSTR and SLRSTR, and enter the values. For those species with missing unary parameters, Aspen Plus online help suggests using the values: SLTSTR = 415 K, SLPSTR = 3000 bar; and SLRSTR = 736 kmol/cum (which must be converted to a mass-based unit with the molecular weight of the component).

Parameters	Units	Data set	Component TICL4	Component TEAL	Component CH4	Component C2H6	Component HX	Component N2	Component C4H10	Component R-C2H4	Component R-C4H8	Component C2H4	Component C4H8	Component H2
SLTSTR	K	1	924.87	924.87	224	315	483.13	140.77	412.78	663.15	924.87	333	396.62	45.89
SLPSTR	bar	1	4000	4000	2482	3273	2900	1786.17	3257.9	4000	4000	2400	2900	1000
SLRSTR	kg/cum	1	866.97	866.97	500	640	786	922.5	755.68	896.6	866.97	631	671.5	142.66

Figure 2.31 Entering unary or pure component parameters of the POLYSL EOS for simulating a HDPE process

To apply the POLYSL EOS to mixtures, the model parameters become composition-dependent through the following mixing rules. The mixing rule for the characteristic closed-packed molar volume of “mers” (that is, the broken parts of a component within a lattice [20]) of the mixture, v_{mix}^* , is

$$v_{mix}^* = \sum_i \sum_j \phi_i \phi_j v_{ij}^* \quad (2.18)$$

with

$$v_{ij}^* = \frac{1}{2} [v_{ii}^* + v_{jj}^*] (1 - \eta_{ij}) \quad (2.19)$$

where the binary interaction parameter η_{ij} (called parameter SLETIJ-1 within Aspen Plus) corrects for deviations from arithmetic mean and where subscripts i and j are the components in the solution mixture. The segment fraction of component i , ϕ_i , is defined as

$$\phi_i = \frac{\frac{w_i}{\rho_i^* v_i^*}}{\sum_j \left(\frac{w_j}{\rho_j^* v_j^*} \right)} \quad (2.20)$$

where w_i is the mass fraction of component i in the mixture, and ρ_j and v_j are the characteristic mass density and closed-packed molar volume of component j , respectively. The mixing rule for the characteristic interaction energy for the mixture, ε_{mix}^* , is

$$\varepsilon_{mix}^* = \frac{1}{v_{mix}^*} \sum_i \sum_j \phi_i \phi_j \varepsilon_{ij}^* v_{ij}^* \quad (2.21)$$

with

$$\varepsilon_{ij}^* = \sqrt{\varepsilon_{ii}^* \varepsilon_{jj}^*} (1 - k_{ij}) \quad (2.22)$$

where ε_{ii}^* and ε_{jj}^* are the characteristic interaction energies between different broken parts of a component within a lattice (called mer-mer interaction in [20]) for components i and j . The binary interaction parameter k_{ij} (called parameter SLKIJ-1 within Aspen Plus) accounts for specific binary interactions between components i and j . Lastly, the mixing rule for the number of sites occupied by a molecule of the mixture, r_{mix} is given by

$$\frac{1}{r_{mix}} = \sum_j \frac{\phi_j}{r_j} \quad (2.23)$$

where r_j is the number of site molecule j occupies in the lattice, and ϕ_j is the segment fraction of component j , defined previously in Eq. (2.20).

Binary interaction parameters k_{ij} and η_{ij} are typically correlated as a function of reduced temperature, $T_r (= T/T_{ref}$ where $T_{ref} = 298.15$ K):

$$k_{ij} = a_{ij} + \frac{b_{ij}}{T_r} + c_{ij} \ln T_r + d_{ij} T_r + e_{ij} T_r^2 \quad (2.24)$$

$$\eta_{ij} = a'_{ij} + \frac{b'_{ij}}{T_r} + c'_{ij} \ln T_r + d'_{ij} T_r + e'_{ij} T_r^2 \quad (2.25)$$

Figures 2.32 and 2.33 shows the values of binary interaction parameters k_{ij} and η_{ij} for simulating a HDPE process [28]. To enter these values within Aspen Plus, follow the path: Properties -> Methods -> Parameters -> Binary Interaction-> New -> Name: SLKIJ-1 -> Enter the values (do the same for SLTIJ-1).

Component i	Component j	Source	Temperature units	AU	B	BU	CU	DU	EU	TREF
C2H4	C4H8	USER	K	0.0248	0	0	0	0	0	298.15
C2H4	HX	USER	K	0.0248	0	0	0	0	0	298.15
C4H8	HDPE	USER	K	0.0208	0	0	0	0	0	298.15
HX	HDPE	USER	K	-0.14	0	0	0	0	0	298.15
CH4	HX	USER	K	0.01951	0	0	0	0	0	298.15
C2H6	HX	USER	K	0.00853	0	0	0	0	0	298.15
H2	HX	USER	K	0.100705	0	0	0	0	0	298.15
C4H10	HX	USER	K	-0.002286	0	0	0	0	0	298.15

Figure 2.32 Binary interaction on parameters k_{ij} for simulating a HDPE process

Component i	Component j	Source	Temperature units	AU	B	BU	CU	DU	EU	TREF
C2H4	C4H8	USER	K	0.0248	0	0	0	0	0	298.15
C2H4	HX	USER	K	0.0248	0	0	0	0	0	298.15
C4H8	HDPE	USER	K	0.0208	0	0	0	0	0	298.15
HX	HDPE	USER	K	-0.14	0	0	0	0	0	298.15
CH4	HX	USER	K	0.01951	0	0	0	0	0	298.15
C2H6	HX	USER	K	0.00853	0	0	0	0	0	298.15
H2	HX	USER	K	0.100705	0	0	0	0	0	298.15
C4H10	HX	USER	K	-0.002286	0	0	0	0	0	298.15

Figure 2.33 Binary interaction on parameters η_{ij} for simulating a HDPE process

2.7 Workshop 2.3 Estimating Property Parameters Using Data Regression Tool

2.7.1 Objective:

This workshop demonstrates how to use the data regression (DRS) tool to identify the pure component parameters and binary interaction parameters of an EOS model based on component liquid density data and binary vapor-liquid equilibrium (VLE) data (two of the most commonly used property data for property parameter regression). We use the example of a slurry HDPE process [28].

We show how to apply the DRS tool according to the following steps: (1) defining a DRS run; (2) specify the unit set and global options; (3) define components, segments, oligomer and polymer, making sure to

define a polymer as an oligomer; (4) choose property method and enter known property parameters from Aspen enterprise databanks; (5) enter experimental data; (6) specify a regression run and physical property parameters to be regressed (7) running the simulation, examining the results and compare the model predictions with experimental data.

2.7.2 Defining a DRS Run

We begin by creating a data regression run and save the simulation file as: **WS2.3 Estimating Property Parameters Using Data Regression Tool.bkp**. We choose a data regression in the run mode section from the toolbar at the top of the screen, as highlighted in Figure 2.34.

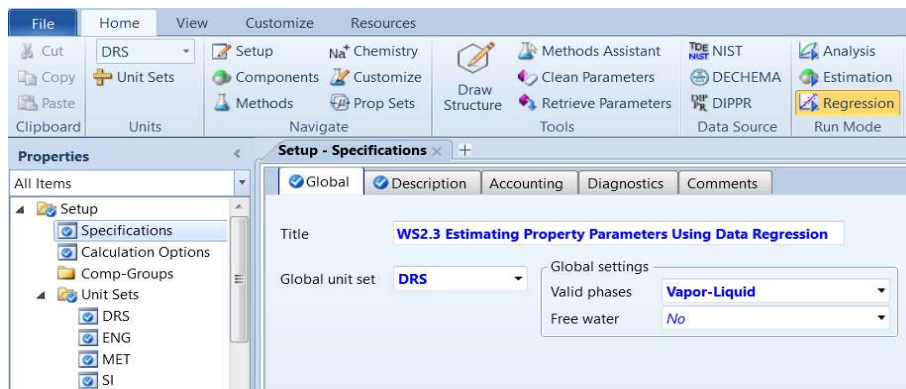


Figure 2.34 Creating a data regression run

2.7.3 Specifying a Unit Set and Global Options

We define a unit set named DRS by copying most units from the unit set, SI, but change the pressure unit to Bar. Following Figure 1.6, we specify a global option of using a mass-based flow rate according to the path: Simulation -> Setup -> Specifications -> Global -> Global settings -> Flow basis: mass.

2.7.4 Defining Components, Segments, Oligomers and Polymer

Figure 2.35 shows the same component specifications for a commercial slurry HDPE process that we will simulate in detail in Chapter 5 [28]. We repeat the important information presented previously in Section 1.3 and emphasize that both property analysis and regression tools in Aspen Plus do **not** support polymer attributes. Therefore, for property analysis and regression runs, we should define a polymer as an oligomer. By doing so, we eliminate the need to enter any attribute information.

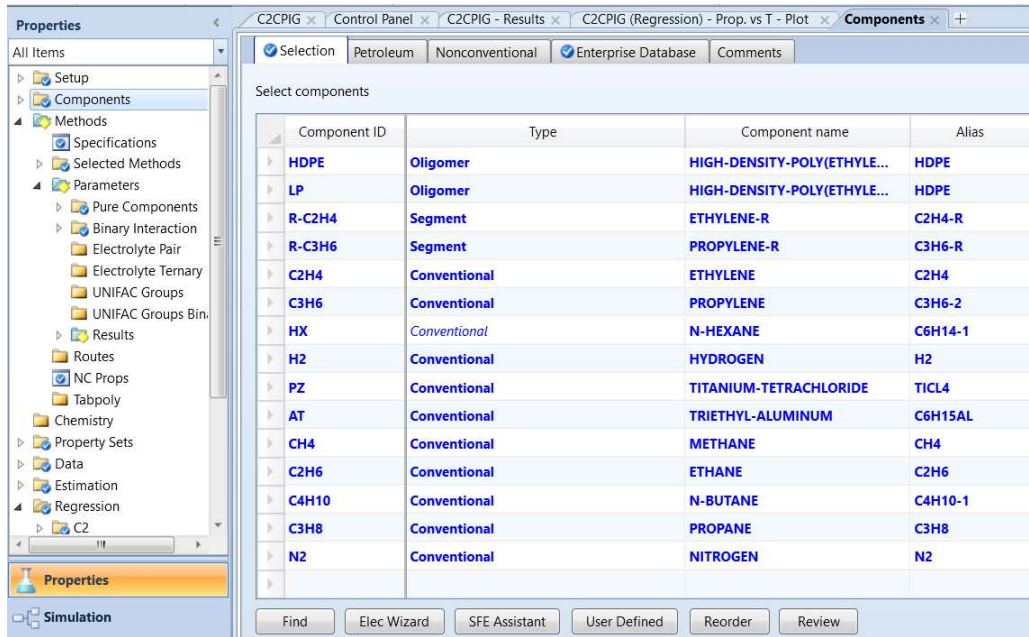


Figure 2.35 Component specifications for data regression of a HDPE process

In the figure, LP refers to an oligomer product; R-C2H4 and R-C3H6 are ethylene and propylene segments; C2H4 and C3H6 are monomer and co-monomer; hexane (HX) is a solvent; H2 is the chain transfer agent; CH4, C2H6, C4H10, and C3H8 are impurities; N2 is an inert gas.

We note that except for HDPE and LP, Aspen Plus automatically fills in the molecular structures for other components that appear in the enterprise databases for pure components and segments. See: Properties-> Components -> Molecular Structure -> Choose component name -> Structural and functional group -> Graphical structure.

We quantify both HDPE and LP by following the path: Properties -> Components ->Polymers -> Segments: Set both segments R-C2H4 and R-C3H6 as repeat unit; and Oligomers: Assume HDPE and LP to have 1500 and 16 repeat segments. Note that the exact number of repeated segments for HDPE does not affect the regression results.

2.7.5 Choose Property Method and Enter Known Property Parameters from Aspen Enterprise Databanks

Clicking on the “Review” button at the bottom of Figure 2.35 will ask Aspen Plus to call up all the relevant pure component parameters from the enterprise databanks for pure components, segments, and polymers. For example, Figure 2.36 shows the resulting listing of pure component parameters (both scalar and temperature-dependent) provided by the databanks. The figure displays the parameters for the ideal gas heat capacity from the segment databank, DB-SEGMENT. To see the specific form of any temperature-dependent parameter correlation, such as CPIG, click the “Help” button in Figure 2.36 to access the Aspen Plus online help. We see the following correlation for CPIG in Figure 2.37.

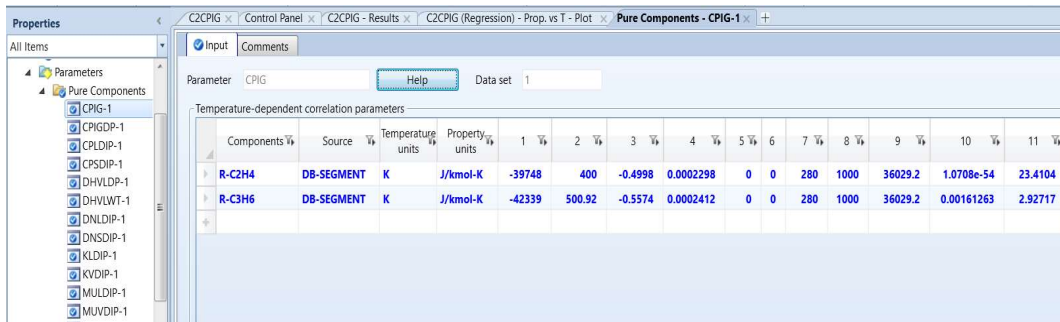


Figure 2.36 Calling up databank values of pure component parameters.

Aspen Ideal Gas Heat Capacity Polynomial

The ideal gas heat capacity polynomial is available for components stored in ASPENPCD, AQUEOUS, and

$$C_p^{*,ig} = C_{1i} + C_{2i}T + C_{3i}T^2 + C_{4i}T^3 + C_{5i}T^4 + C_{6i}T^5 \text{ for } C_{7i} \leq T \leq C_{8i}$$

$$C_p^{*,ig} = C_{9i} + C_{10i}T^{C_{11i}} \text{ for } T < C_{7i}$$

$C_p^{*,ig}$ is linearly extrapolated using slope at C_{8i} for $T > C_{8i}$.

Parameter Name/Element	Symbol	Default	MDS	Lower Limit	Upper Limit	Units
CPIG/1	C_{1i}	—	—	—	—	MOLE-HEAT-CAPACITY, TEMPERATURE
CPIG/2, ..., 6	C_{2i}, \dots, C_{6i}	0	—	—	—	MOLE-HEAT-CAPACITY, TEMPERATURE
CPIG/7	C_{7i}	0	—	—	—	TEMPERATURE
CPIG/8	C_{8i}	1000	—	—	—	TEMPERATURE
CPIG/9, 10, 11	C_{9i}, C_{10i}, C_{11i}	—	—	—	—	MOLE-HEAT-CAPACITY, TEMPERATURE †

Figure 2.37 Access Aspen Plus online help for CPIG parameter correlation

Additionally, we can see the scalar pure-component parameter values by following the path: Properties->Methods->Parameters->Pure components->REVIEW-1. See Figure 2.38. To understand the meaning of each listed parameter, click on the name to expand the pull-down menus, you will see a description.

Parameters	Units	Data set	Component	Component	Component	Component	Component
			C2H4	C3H6	HX	H2	PZ
API		1	265.5	139.6	81.6	340	-49.274
CRITMW		1					
DCPLS	J/kmol-K	1		29301.9	43537.9	6892.2	18686.
DELTA	(J/cum)**.5	1	11869.8	12702.6	14880	6650.04	1827
DGFORM	J/kmol	1	6.844e+07	6.264e+07	-66340	0	-7.267e+0
DGFORM	J/kmol	1	5.251e+07	2.023e+07	-1.6694e+08	0	-7.6166e+0
DGFVKM	J/kmol	1	1.34871e+07	1.87317e+07	2.88018e+07	896545	3.40085e+0
DGSFRM	K	1	104	87.9	177.83	13.95	249.0

Figure 2.38 Values of scalar pure component parameters called up from the databanks and displayed in REVIEW-1

For HDPE, Aspen Plus assume the molecular weight for HDPE to be that of the C2H4 segment, that is, 28.0538. To enter the correct molecular weight of our HDPE “oligomer” with 1500 repeated segments, we follow the path: Properties -> Methods -> Parameters -> Pure Components -> New -> Name: MWHDPPE -> Input: Component = HDPE, Parameter: MW= 42080.7(= 28.0538 x 1500). We note that the exact value of this MW does not affect the regression results.

This list of pure component parameters displayed by Aspen Plus in Figure 2.38 does not include the values of T^* , P^* and ρ^* defined by Eq. (2.17) and illustrated in Figure 2.31. We follow the path: Properties -> Methods -> Parameters -> Pure Components -> New: name = SLTPR -> Parameters: SLTSTR, SLPSTR and SLRSTR, and enter the values according to [28]. See Figure 2.39. These values are essential when running regression of vapor-liquid equilibrium data for missing binary interaction parameters.

Parameters	Units	Data set	Component R-C2H4	Component C2H4	Component AT	Component PZ	Component HX	Component R-C3H6	Component C4H10	Component C3H6	Component H2	Component N2	Component CH4	Component C3H8
SLTSTR	K	1	663.15	333	924.87	924.87	483.13	724.3	412.78	360.43	45.89	140.77	224	354.33
SLPSTR	bar	1	4000	2400	4000	4000	2900	2800	3257.9	3100	1000	1786.17	2482	2800
SLRSTR	kg/cum	1	896.6	631	866.97	866.97	786	938.87	755.68	670.83	142.66	922.5	500	615.91

Figure 2.39 Pure component parameters for POLYSL EOS for a HDPE process

2.7.6 Enter Experimental Data for Data Regression, Run the Regression and Examine the Results

We first demonstrate how to regress the pure component parameters for POLYSL, T^* , P^* and ρ^* , defined by Eq. (2.17) for C2H4, and compare with the resulting values with those listed in Figure 2.39. We enter the liquid density data of C2H4 [32] by following the path: Properties -> Data -> New -> Enter ID: C2RHOL, select type: PURE-COMP -> Setup: Category = Thermodynamic, Property = RHOL, Component = C2H4; Data – enter C2RHOL data according to Figure 2.40. To enter the TPXY data of Figure 2.41, we follow the path: Properties ->Data ->New ->Enter ID: PEXY1, select type: MIXTURE ->Setup: Category ->Phase Equilibrium, Data type ->TPXY, Components in mixture: C2H4, HDPE, Composition basis: Mass fraction, Data-> enter the data displayed in Figure 2.41.

Usage	TEMPERATURE K	PRESSURE kPa	RHOL kg/cum
STD-DEV	0.1	0.1%	1%
DATA	169.43	101.3	567.92
DATA	183	213	547.95
DATA	193	341	532.88
DATA	203	518	517.17
DATA	213	755	500.61
DATA	223	1063	482.84
DATA	233	1453	463.41
DATA	243	1938	441.61
DATA	263	3240	385.64
DATA	281	4899	287.43

Figure 2.40 Liquid density data for C2H4 for regression of pure component parameters

Usage	TEMPERATURE K	PRESSURE bar	X HDPE	X C2H4	Y HDPI	Y C2H4
STD-DEV	0.1	0.1%	0.1%	0	1%	0
DATA	399.15	455.8	0.9982	0.0018	0	1
DATA	399.15	790.3	0.9963	0.0037	0	1
DATA	399.15	1135	0.9945	0.0055	0	1
DATA	399.15	1479	0.9925	0.0075	0	1
DATA	399.15	1824	0.9893	0.0107	0	1
DATA	399.15	2168	0.9864	0.0136	0	1
DATA	399.15	2513	0.9842	0.0158	0	1
DATA	399.15	2847	0.9825	0.0175	0	1
DATA	399.15	3202	0.9802	0.0198	0	1
DATA	399.15	3546	0.9779	0.0221	0	1
DATA	399.15	3891	0.9758	0.0242	0	1
DATA	399.15	4235	0.9745	0.0255	0	1
DATA	399.15	4580	0.9715	0.0285	0	1
DATA	399.15	4924	0.9695	0.0305	0	1
DATA	399.15	5269	0.967	0.033	0	1
DATA	399.15	5613	0.9641	0.0359	0	1

Figure 2.41 TPXY data for regression of binary interaction parameters

2.7.7 Specifying a Regression Run and the Parameters to be Regressed

To regress the pure component parameters for POLYSL, we follow the path: Properties -> Regression -> New: Enter ID = C2 -> Input: see Figure 2.42.

Data set	Weight	Consistency	Reject data	Test method	Area tolerance %	Point tole
C2RHOL	1	<input type="checkbox"/>	<input type="checkbox"/>	Area tests	10	

Figure 2.42 Input for regressing pure component parameters using liquid density data C2RHOL

Next, we specify the pure component parameters to be regressed. See Figure 2.43.

Type	Parameter	Parameter	Parameter
Name	SLTSTR	SLPSTR	SLRSTR
Element			
Component or Group	C2H4	C2H4	C2H4
Usage	Regress	Regress	Regress
Initial value	300	2e+08	500
Lower bound	300	2e+08	500
Upper bound	1000	4e+08	1000
Scale factor	1	1	1
Set Aji = Aij	No	No	No

Figure 2.43 Specification of POLYSL pure component parameters to be regressed

2.7.8 Running the Regression Case and Examining the Results

When running the regression, the control panel first shows which regression case to run. We choose case C2 and click OK to run. See Figure 2.44.

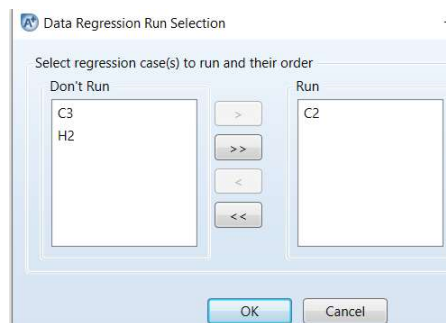


Figure 2.44 Selecting the regression case C2 to run

We follow Figure 2.45 to keep the regressed pure component parameter values in the result folder of regression run C2 and not replace the previously entered values. See Figure 2.46. *The regressed parameters $SLTSTR = 334.509$ K, $SLPSTR = 2.39886E8$ kPa = 2398.86 bar, and $SLRSTR = 631.704$ kg/cum, which compare favorably with the values of 333, 2400 and 631 entered for C2H4 in Figure 2.39 [28].* Looking at “Profiles” folder of results, we see a table of comparison of experimental and estimated values of temperature, pressure, and liquid density of C2H4. See Figure 2.47. We plot the results by following the path: Plot (upper right corner of the computer screen) -> Custom -> X-axis: Exp Val RHO LIQUID C2H4, kg/cum; Y-axis: Est Val RHO LIQUID C2H4, kg/cum. See the initial plot in Figure 2.48 -> Plot: Format. Choose Squared plot and Diagonal line -> see the improved plot in Figure 2.49.

We can use the same approach to regress the pure component parameters for the ethylene segment and other components using the liquid density data. Experimental data for liquid density and heat capacity for most components in the PE, HDPE, LDPE and LLDPE processes are available in [32 to 37].

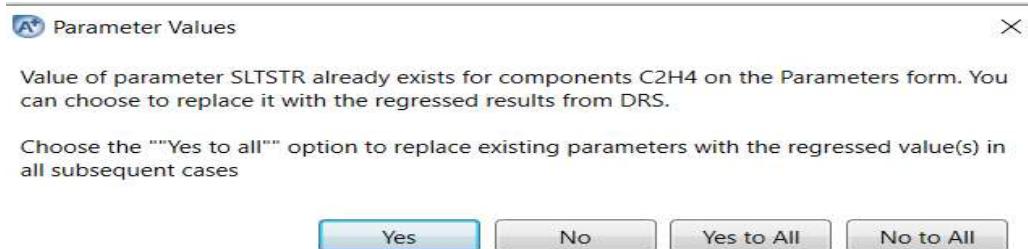


Figure 2.45 Clicking No three times for not placing the parameter values of SLTSTR, STPSTR and SLRSTR previously entered in Figure 2.39.

Parameter	Component i	Component j	Value (SI units)	Standard deviation
SLTSTR/1	C2H4		334.508	3.53568
SLPSTR/1	C2H4		2.39886e+08	5.22819e+06
SLRSTR/1	C2H4		631.704	2.53172

Figure 2.46 Regressed values of POLYSL pure component parameters for C2H4

	Exp Val TEMP	Est Val TEMP	Exp Val PRES	Est Val PRES	Exp Val RHO LIQUID C2H4	Est Val RHO LIQUID C2H4
	K	K	bar	bar	kg/cum	kg/cum
	169.43	169.429	1.013	1.013	567.92	564.137
	183	183	2.13	2.13	547.95	547.494
	193	193.001	3.41	3.41	532.88	533.808
	203	203.001	5.18	5.18	517.17	518.791
	213	213.001	7.55	7.55	500.61	502.287
	223	223.001	10.63	10.63	482.84	484.083
	233	233.001	14.53	14.53	463.41	463.865
	243	242.999	19.38	19.38	441.61	441.165
	263	262.996	32.4	32.4001	385.64	384.401
	281	281.002	48.99	48.9898	287.43	287.461

Figure 2.47 Comparison of experimental and estimated temperature, pressure, and liquid density of C2H4.

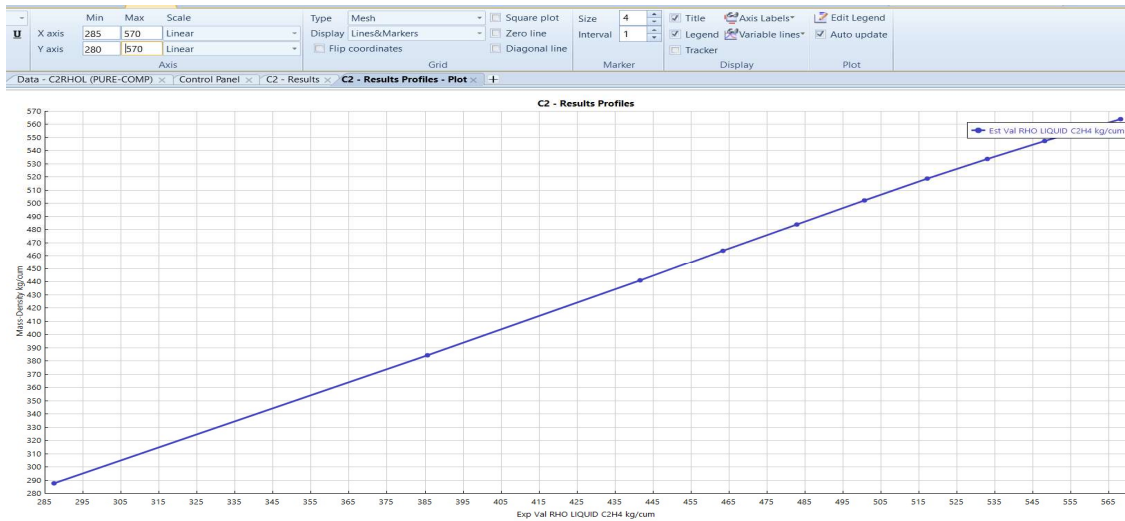


Figure 2.48 The initial plot of estimated liquid density of C2H4 value versus measured value. Note the Format options of Squared plot and Diagonal line at the top.

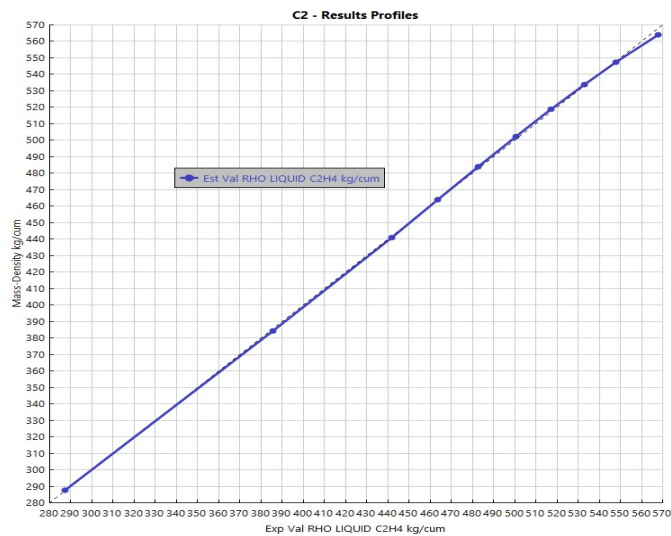


Figure 2.49 Improved plot of estimated versus measured liquid density of C2H4.

Next, we demonstrate how to regress binary interaction parameters SLETIJ (η_{ij}) and SLKIJ (k_{ij}) based on Eqs. (2.24) and (2.25) using the liquid density data of C2H4, C2RHOL, of Figure 2.40 and the vapor-liquid equilibrium data for polyethylene and ethylene, PEXY1, of Figure 2.41.

We create a new regression run by following the path: Properties -> Regression -> New -> Enter ID: C2TPXY->OK -> Setup: enter datasets PEXY1 and C2RHOL (following Figure 2.42) -> Parameters -> See Figure 2.50 for specifying the binary interaction parameters to be regressed.

Parameters to be regressed		
Type	Binary parameter	Binary parameter
Name	SLETIJ	SLKIJ
Element	1	1
Component or Group	C2H4	C2H4
Usage	Regress	Regress
Initial value	0.03	0.25
Lower bound	0.012	0.16
Upper bound	1	1
Scale factor	1	1
Set Aji = Aij	No	No

Figure 2.50 Specification of binary interaction parameters to be regressed

Following Figures 2.44 to 2.46, we run the regression case C2TPXY, and the resulting binary interaction parameters appear in Figure 2.51. The accuracy of these parameters depends on the accuracy of the experimental data.

Parameter	Component i	Component j	Value (SI units)	Standard deviation
SLETIJ/1	C2H4	HDPE	0.012	0
SLKIJ/1	C2H4	HDPE	0.219778	0.0219851

Figure 2.51 Regressed binary interaction parameters between C2H4 and HDPE.

2.8 Polymer Perturbed-Chain Statistical Fluid Theory (POLYPCSF) Equation of State

Gross and Sadowski [21 to 23] developed the PC-SAFT EOS, which is an extension of the well-known SAFT EOS [24 to 26]. A key difference between the two models is that PC-SAFT model replaces the expression of the dispersion (attractive) interactions between isolated (or disconnected) polymer segments with that between connected polymer segments. See an illustration in Figure 2.52, in which each circle dot represents a segment.

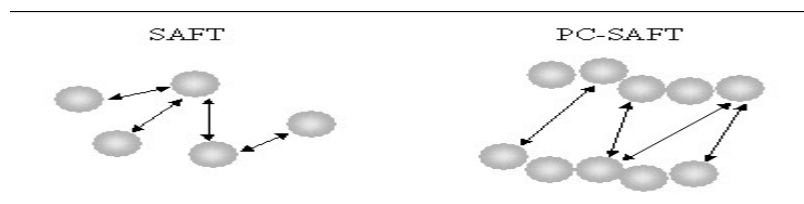


Figure 2.52 An illustration of the disconnected segments in SAFT versus the connected segments in PC-SAFT.

The PC-SAFT model is applicable to fluid systems of both small and large molecules over a wide range of temperature and pressure conditions, and it represents polymer systems very well.

Statistical thermodynamics typically uses the Helmholtz free energy A to represent the attractive (or perturbation) interactions between molecules, as most properties of interest, such as pressure, can be obtained by proper differentiation of A . In the SAFT model, this attractive or perturbation term is a

series expansion in terms of the reciprocal temperature, and each coefficient of the expansion depends on the density and composition. By contrast, the PC-SAFT model represents the molar residual Helmholtz free energy A^{res} as a sum of two contributions

$$A^{res} = A^{ref} + A^{pert} \quad (2.26)$$

where A^{res} and A^{pert} are the reference and perturbation (attractive) contributions, respectively. The reference term considers a fluid consisting of hard-sphere chains as a reference for the perturbation theory, and the perturbation term incorporates the attractive forces between the chains.

The primary difference between the PC-SAFT and SAFT models is in the perturbation term. The SAFT model uses hard spheres, not hard-sphere chains, as a reference fluid for the perturbation contribution. The use of hard-sphere chains allows the PC-SAFT EOS to account for the connectivity of segments that comprise the chains when considering the attractions between species, resulting in a more realistic description of the thermodynamic behavior of mixtures of chainlike molecules. Gross and Sadowski [21 to 23] and others [e.g., 29 to 31] demonstrate that the PC-SAFT predictions for vapor-liquid and vapor-liquid-liquid equilibria are superior to the SAFT model.

The resulting PC-SAFT EOS expresses the compressibility as a sum of the ideal (with a value of unity), reference and perturbation contributions:

$$\frac{PC}{RT} = z = z^{id} + z^{ref} + z^{pert} = 1 + z^{ref} + z^{pert} \quad (2.27)$$

Interested readers may refer to the original references for the analytical expressions of the PC-SAFT model [21 to 23] for the details of these contributions. A recent article by Kang et al. [27] gives a fairly complete analysis of the PC-SAFT model equations and their iterative solution procedures.

The application of the PC-SAFT model requires the use of three pure-component parameters for each species involved: (1) *segment number*, m , which is a characteristic length and is directly proportional to the size (molecular weight) of the species; (2) *segment diameter*, σ Å; and (3) *segment energy*, ϵ Joule, typically expressed as a ratio ϵ/k_B in K, where k_B is the Boltzmann's constant, 1.38×10^{-23} J/K. For polymers, we typically replace the segment number m by a ratio r defined as m divided by the number-average molecular weight, MWN:

$$r = m / MWN \quad (2.28)$$

Using this ratio is more convenient because the polymer molecular weight is often unknown until the polymer is produced. For segments, we often use the ratio r as well. These parameters are obtained by fitting experimental vapor pressure and liquid molar volume data for pure components.

Figure 2.53 illustrates the values of these pure component parameters in the simulation of a gas-phase PP process [42]. To enter these parameters in Aspen Plus, follow the path: Properties -> Methods -> Parameters -> Pure Components -> New: name = PCSAFT -> Enter parameter name, component, and value. In the figure, (1) parameter PCSFTM is the segment number m ; (2) parameter PCSFTU represents the ratio of the segment energy to the Boltzmann's constant ϵ/k in K; (3) parameter PCSFTV is the segment diameter, σ Å; and (4) parameter PCSFTR represents the ratio r in mol/g defined by Eq. (2.27). For those species with missing pure component parameters, a search "missing parameters (POLYPCSF)" of Aspen Plus online help suggests using the values: PCSFTM = 0.02434*(component molecular weight); PCSFTU = 267.67 K; PCSFTV = 4.072 Å; and PCSFTR = 0.02434 mol/g for polymer species and segments.

Parameters	Units	Data set	Component CAT	Component COCA	Component H2	Component ETHYLEN	Component ETHANE	Component O2	Component PROPEN	Component PROPAN	Component DIBDI	Component C3-SEG	Component C2-SEG
PCSFTM		1	25	25	0.828469	1.55873	1.6068	1.7677	1.9598	2.002	25		
PCSFTU	K	1	198.821	198.821	12.5276	179.412	191.42	83.6089	207.19	208.11	198.821	298.639	252
PCSFTV		1	2.66798	2.66798	2.97294	3.43405	3.5206	3.1191	3.5356	3.6184	2.66798	4.14728	4.0217
PCSFTR		1										0.025279	0.0263

Figure 2.53 Pure component parameters for POLYPCSF model for simulating a PP process.

The POLYPCSF model also requires binary interaction parameters that are correlated by Eq. (2.24) as a function of $T_r (= T/T_{ref}$ where $T_{ref} = 298.15$ K):

$$k_{ij} = a_{ij} + \frac{b_{ij}}{T_r} + c_{ij} \ln T_r + d_{ij} T_r + e_{ij} T_r^2 \quad (2.24)$$

These parameters may be obtained by regressing phase-equilibrium data. When these parameter values are not supplied, they default to zero.

2.9 Workshop 2.4 Regression of Property Parameters for POLYPCSF EOS

2.9.1 Objective and Data Sources:

The objective of this workshop is to demonstrate the step-by-step procedure of Workshop 2.3 for regression of property parameters the POLYSL EOS is directly applicable to the POLYPCSF EOS.

For polymer components, we may find relevant thermophysical property and phase equilibrium data: (1) for ethylene and propylene in [35,36,37]; (2) for polymer solutions and components in [32,33,38,39,41]; (3) for solvent vapor and liquid phase data in [34]; and (4) for pure component parameters for POLYPCSF for PP process in [42].

2.9.2 Regression of Pure Component Parameters for POLYPCSF EOS

Following Figure 2.34, we begin by creating a data regression run and choosing the MET unit set and save the simulation file as: **WS2.4 Regressing Property Parameters for POLYPCSF.bkp**.

Figure 2.54 shows the component specification. As discussed in Sections 2.7.4, both property analysis and regression tools in Aspen Plus do *not* support polymer attributes. Therefore, for property analysis and regression runs, we define PE as an oligomer.

Component ID	Type	Component name	Alias
PE	Oligomer	POLY(ETHYLENE)	PE
C2H4	Conventional	ETHYLENE	C2H4
C2H4SEG	Segment	ETHYLENE-R	C2H4-R

Figure 2.54 Component specifications.

We follow the path: Properties -> Components -> Polymers -> Characterization: (1) Segments – Define C2H4SEG as repeat segment; (2) Oligomers: Specify PE to include 1250 C2H4SEG. Next, we click on “Review” button illustrated in Figure 2.54 to call up pure component parameters from Aspen Plus databanks for pure components, segments and polymers. Following the path: Properties -> Parameters -> Pure Components -> REVIEW-1 -> we see in Figure 2.55 the molecular weight (MW) for PE being 28.0538, which is the molecular weight of the monomer C2H4, not that of the oligomer with 1250 C2H4SEG repeated segments. To specify the correct molecular weight of PE, we follow the path: Properties -> Parameters -> Pure Components -> New -> Choose type = scalar and specify name = MWPE -> OK -> Input: enter component PE, parameter MW =35067.25 (28.0538 x 1250).

Parameters	Units	Data set	Component	Component	Component
API		1	265.5		
CRITMW		1		3500	
DGFORM	cal/mol	1	16346.6		
DHFORM	cal/mol	1	12541.8		
DHVLB	cal/mol	1	3221.34		
FREEZEPT	K	1	104		
HCOM	cal/mol	1	-315993		
HFUS	cal/mol	1	800.373		
MUP	debye	1	0		
MW		1	28.0538	28.0538	28.0538
OMEGA		1	0.0862484	0	

Figure 2.55 Pure component parameters from Aspen databanks

We follow the procedure in Figure 2.40 to enter the liquid density dataset PERHOL for PE (see Figure 2.56), and to enter the vapor-liquid equilibrium dataset PETPXY1 for C2H4-PE of Figure 2.41 (with component name PE replacing HDPE).

Usage	TEMPERATURE	RHOL
	C	kg/cum
STD-DEV	0.1	1%
DATA	135.1	787.9
DATA	142.7	783.58
DATA	149.5	779.61
DATA	160.5	773.4
DATA	172	767.05
DATA	184.8	760.05
DATA	198	753.38

Figure 2.56 Liquid density dataset PERHOL of PE

Following Figure 2.42, we set up a regression run C2H4SEG to estimate the POLYPCSF pure component parameters PCSFTU (the ratio of the segment energy to the Boltzmann’s constant ϵ/k in K), PCSFTV (the segment diameter, σ Å), and PCSFTR (the ratio r in mol/g defined by Eq. (2.27)) for C2SEG. See Figure 2.57.

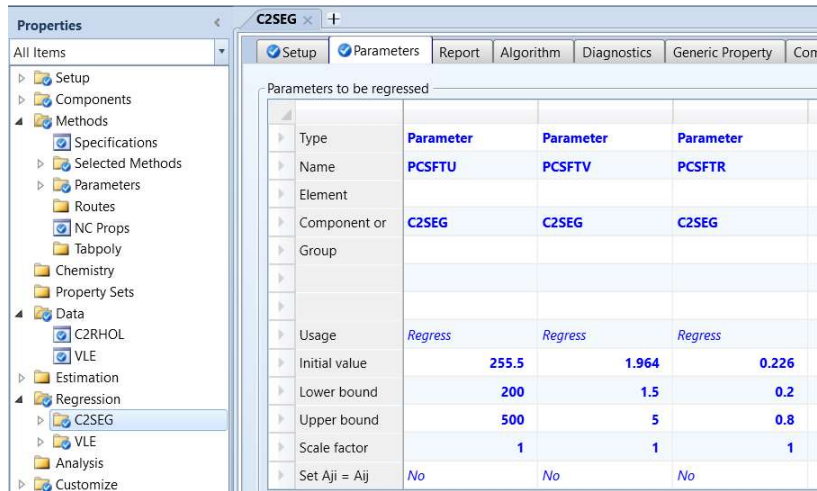


Figure 2.57 Setting up a regression run for POLYPCSF pure component parameters of C2SEG

Executing a regression run based on the liquid density dataset C2RHOL gives the resulting pure component parameters of Figure 2.58.

Parameter	Component i	Component j	Value (SI units)	Standard deviation
PCSFTU/1	C2H4SEG		254.445	1.95559
PCSFTV/1	C2H4SEG		1.94588	0.0778691
PCSFTR/1	C2H4SEG		0.232374	0.0278565

Figure 2.58 Regressed POLYPCSF pure component parameters for C2H4 Segment

The last two columns in Figure 2.59 show that the estimated liquid density data of PE match the experimental data well.

Exp Val TEMP	Est Val TEMP	Exp Val PRES	Est Val PRES	Exp Val RHO LIQUID PE	Est Val RHO LIQUID PE
K	K	atm	atm	kg/cum	kg/cum
408.25	408.25	1	1	787.9	787.733
415.85	415.85	1	1	783.58	783.457
422.65	422.65	1	1	779.61	779.658
433.65	433.65	1	1	773.4	773.56
445.15	445.15	1	1	767.05	767.238
457.95	457.95	1	1	760.05	760.248
471.15	471.15	1	1	753.38	753.08

Figure 2.59 A comparison of estimated and experimental data of liquid density data of PE.

Following Figure 2.50, we create a regression run BINARY to estimate the binary interaction parameter PCSKIJ between components C2H4 and C2H4SEG using the vapor-liquid equilibrium dataset PETPXY1 for C2H4-PE of Figure 2.41 (with component name PE replacing HDPE). See Figure 2.60.

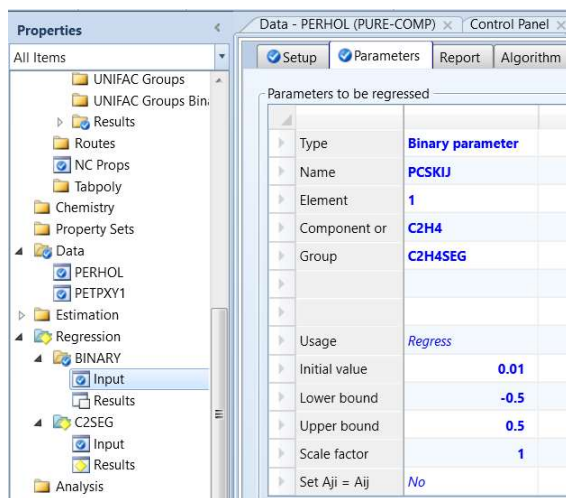


Figure 2.60 Input to regress binary interaction parameter PCSKIJ

Figure 2.61 shows the resulting binary interaction parameter. This concludes the current workshop. We save the simulation file as **WS 2.4 Regressing Property Parameters for POLYPCSF.bkp**.

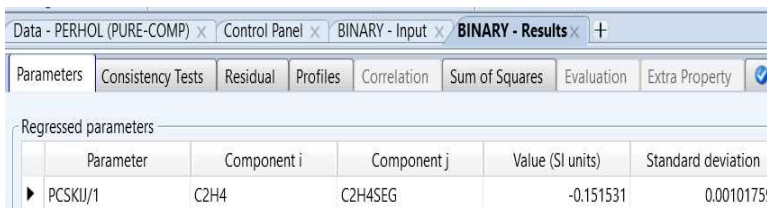


Figure 2.61 Regressed POLYPCSF binary interaction parameter

This workshop concludes our sections of selection of thermodynamic methods and estimation of physical properties. We summarize our discussion of the differences between an equation of state (EOS) and an activity coefficient (gamma) model for polymer applications in Table 2.6.

Table 2.6 Comparison of an equation of state and an activity coefficient model for polymer applications

EOS Models	Gamma or Activity Coefficient Models
Limited in ability to represent nonideal liquid	Can represent highly nonlinear liquids with polar and hydrogen-bonding species
Fewer binary interaction parameters required	Many binary interaction parameters required; Section 2.3
Parameters extrapolate reasonably with temperature	Binary interaction parameters are highly temperature-dependent
Can represent both vapor and liquid	Can only represent the liquid phase
Consistent in critical region for light gases and low-molecular weight components	Inconsistent in critical region, resulting in incorrect concentrations of light gases and low-molecular weight components in liquid phase, Section 2.2.5

Common EOS Models	Common Gamma Models
POLYSL, Polymer Sanchez-Lacombe EOS, Sections 2.6 and 2.7; POLYPCSF, Polymer Perturbed-Chain Statistical Fluid Theory EOS, Sections 2.8 and 2.9	POLYNRTL, Polymer Non-Random Two-Liquid Activity Coefficient Model, Sections 2.2.4 and 2.3

2.10 Correlation of Polymer Product Quality Indices and Structure-Property Correlations

2.10.1 Polyolefin Product Quality Indices

Fundamentally speaking, polymer products are characterized by their molecular structures. The key quality measures include molecular weight averages (MWN and MWW), polydispersity index, copolymer composition, type and frequency of branching, tacticity, etc. Aspen Polymers can predict these quality indices from the moment equations as a part of the simulation model.

In practice, industrial polymer producers focus more on empirical product quality indices. Two most important quality measures are *melt index (MI)* or *melt flow rate (MFR)*, and *polymer density*. MI or MFR is defined as the mass of polymer, in grams, flowing in ten minutes (gm/10 min) through a capillary of a specific diameter and length by a pressure applied via prescribed alternative gravimetric weights for alternative prescribed temperatures. The standard testing methods are ASTM D1238 for flow rates of thermoplastics by extrusion plastometer, and ISO 1133 for determination of MFR of thermoplastics. For density, the standard testing methods are ASTM D1505 for density of plastics, ASTM D792-00 for density and specific gravity of plastics, and ISO 1183 for density of plastics.

Figure 2.62 illustrates a melt-flow plastometer for MI determination. The polymer melt flows through the barrel, entrance region (or contraction) and capillary. The blow-up depicts the entrance region, where funneling flow takes place. The size of the capillary is standardized at 0.083" diameter and 0.250" length. For polyethylenes, the most common conditions are 190° C and 2.16 kg force. For polypropylene, the temperature is 230°C. For some polyethylene, the load is increased to 21.6 kg, which is called *the High Load Melt Index, (HLMI)* [43]. MI gives a relative indication of the molecular weight and viscosity of the polymer. The lower the MI, the higher the molecular weight and viscosity.

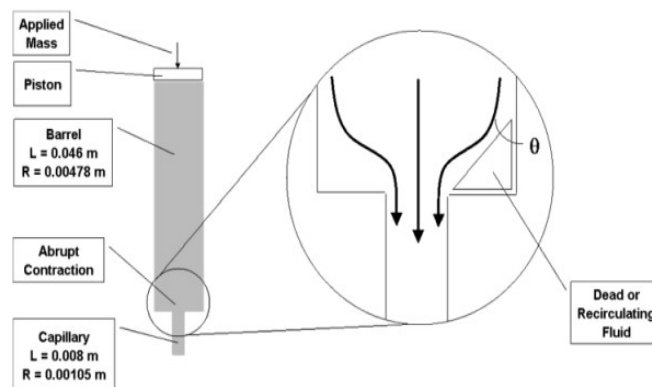


Figure 2.62 Melt-flow plastometer for MI determination.

The tacticity is an important quality measure of polypropylene. In Figure 2.63, we see in an *isotactic* PP, (all the repeating methyl CH₃) groups, represented by the dark downward arrow, are arranged along the same side of the polymer chain. In the *syndiotactic (syntactic)* PP, the repeating methyl groups are arranged on an alternating side of the polymer chain, while in the *atactic* PP, the repeating methyl

groups are on either side of the polymer chain. In Chapter 5, we show that Aspen Polymers simulation quantifies the tacticity of PP by an *atactic fraction (ATFRAC)*, which is defined as the ratio of atactic propagation reaction rate to the total propagation reaction rate.

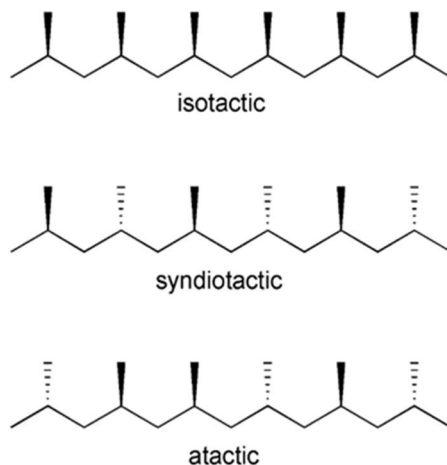


Figure 2.63 Three stereochemical configurations of PP

2.10.2 Empirical Correlations of Polymer Product Quality Targets

We first note that the estimated molecular weight distribution can vary by catalyst, process, plant operation, and testing method. Therefore, empirical correlations of polymer product quality targets have a limited range of applicability. Correlations from a particular catalyst, a particular comonomer, a single reactor, or from multi-reactor operations could be different.

In an early publication in 1953, Sparati, et al. [44] presented a fairly complete study of eleven property correlations of LDPE. Two of the reported correlations include:

$$\text{Log (MI)} = 5.09 - 1.53 \times 10^{-4} (\text{MWN}) \quad (2.29)$$

$$\text{Density} = 2.0 \times 10^{-3} (\text{crystallinity}) + 0.03 \quad (2.30)$$

A popular correlation for HDPE or LLDPE copolymer density is of the form

$$\text{Density} = A - B^*(\text{SFRAC} * 100)^C \quad (2.31)$$

where A, B and C are constants, and SFRAC is the mole fraction of the comonomer in the polymer product (e.g., comonomer 1-butene with monomer ethylene).

In the literature, most empirical correlations for MI for polyolefins with broad MWD or large PDI are based on the weight-average molecular weight (MWW). For example, a general MI correlation with MWW [44 to 46] is in the form of

$$\text{MI} = a(\text{MWW})^{-b} \quad (2.32)$$

where a and b are correlating parameters. For PP, the MI may depend on the MWW as well as the atactic fraction (ATFRAC), calculated by the atactic chain propagation reaction (ATACT-PROP) in Aspen Polymers [42].

The polymer density is usually measured for the pellets and correlated as a function of the MWW. For copolymerization, we often correlate the polymer density as a function of mole fraction of the comonomer and the MWW [46,47]. In reference [47], the HDPE density obtained from ethylene copolymerization with comonomer 1-butene follows the following correlation:

$$(1 - 0.0081x_B^{0.148895})x [1.137247 - 0.014314 \ln(\text{MWW})] \quad (2.33)$$

where x_B is the mole fraction of 1-butene.

We demonstrate below how to develop simple linear and nonlinear correlations of melt index based on the measured data from a PP process using Excel. We save the Excel file as **Example 2.2 Correlation of Melt Index.xlsx**.

	B	C	D	E	F	G	H	I	
1									
2	MI = (a/MWW)^b								
3	use solver to minimize sum of squared errors (SOE)								
4	i. e., SOE = sum((MI-(a/MWW)^b)^2)								
5	by adjusting a and b								
6	MWW=PDI*MWN								
7									
8	Grade 1							b	2.640954
9	MI	MWN	PDI		MWW	(a/MWW)^b	Squared Error	a	2338559.779516
10	175	60000		5.5	330000	176.1809067	1.394540573		
11	155	63000		5.52	347760	153.4036518	2.548327434		
12	115	70000		5.54	387800	115.038746	0.001501253		
13	65	80000		6	480000	65.4942942	0.244326757		
14						SOE	4.188696017		
15	Grade 2							b	3.774509
16	MI	MWN	PDI		MWW	(a/MWW)^b	Squared Error	a	491762.151756
17	1.4	80000		5.6	448000	1.421612106	0.000467083		
18	1.15	83000		5.7	473100	1.157230495	5.22801E-05		
19	0.9	90000		5.8	522000	0.798329336	0.010336924		
20	0.4	96000		6.2	595200	0.486478563	0.007478542		
21						SOE	0.018334829		
22									

Figure 2.64 Using Excel to develop a correlation for melt index

Referring to Figure 2.64, we see the measured data for MI, MWN, and MWW, and PDI (= MWW/MWN) for polymer grade 1 in cells B10 to B13, C10 to C13, E10 to E13 and D10 to D13; and for polymer grade 2 in cells B17 to B20, C17 to C20, E17 to E20 and D17 to D20. Based on assumed values of parameters a and b, we find the sum of squared errors (SOE) between the estimated values and experimental data, and then use Goal Seek solver in Excel to find the fitted values of parameters a and b that minimize the SOE. To access the Goal Seek solver, follow the path: Data -> What-If Analysis -> Goal Seek. We note that because of the significant difference in the values of MI for grades 1 and 2, it may be best to develop two separate correlations for the measured data.

2.10.3 Estimation of Apparent Newtonian Viscosity from MI-MWW Measurement

We begin with some background about Newtonian and non-Newtonian fluids. Newtonian fluids satisfy Newton's law of viscosity, where the proportionality constant η is the viscosity of the fluid.

$$\tau \text{ (shear stress, Pa)} = \eta \text{ (viscosity, Pa-s)} \times \dot{\gamma} \text{ (shear rate, 1/s)} \quad (2.34)$$

In reality, most fluids are non-Newtonian, which means that their viscosity depends on shear rate (shear thinning or thickening) or the deformation history. Non-Newtonian fluids display a nonlinear relation between viscosity and shear rate (see Figure 2.65). A fluid is shear thickening if the viscosity of the fluid increases as the shear rate increases. A common example of shear thickening fluids is a mixture of corn

starch and water. Fluids are shear thinning if the viscosity decreases as the shear rate increases. Common examples include ketchup, paints and blood.

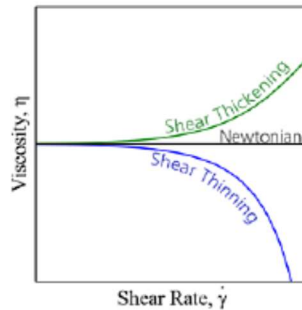


Figure 2.65 An illustration of shear thickening, shear thinning and Newtonian fluid.

Seavey et al. [45] review the relationships among the molecular weight distribution, Non-Newtonian shear viscosity, and melt index. Both simple and more complex semi-empirical methods exist to relate these variables. For example, Bremner et al. [49] present experimental data and study the relationship between different molecular weight averages and melt index for several commercial thermoplastics, including PS, PP, LPDE, and HDPE.

Rohlfing and Janzen [50] take a different approach by using a model for the flow within the melt indexer itself to predict the melt index. Sharma and Liu [53],[54] review the relationship of melt index and molecular weights with input process parameters. Referring to Figure 2.62, they consider the pressure drop in the melt indexer as a sum of the pressure drops in the barrel, entrance region and the capillary. They develop a set of *integral-algebraic equations* relating the shear rates at the barrel wall, at the capillary wall, and in the capillary, the barrel pressure drop, the capillary pressure drop, the entrance pressure drop, and the volumetric flow rate.

For a *Newtonian* fluid with viscosity μ (in Pascal-second, or Pa-s) and based on the melt indexer of Figure 2.62 with standard dimensions specified in Section 2.10.1, analytical solutions of the Rohlfing and Janzen model equations is possible, and it results in a simple equation:

$$MI = 7280/\mu \quad (2.35)$$

The details appear in [45].

Working backwards from the melt index to predict the non-Newtonian shear viscosity (or "flow curve") is difficult because of the integral-algebraic equations involved. In cases where the integral covers part of the shear-thinning region of the flow curve, solutions to the flow model are not unique. For example, a polymer with a high Newtonian viscosity but with a rapid onset of shear thinning may have the same melt index as a polymer with a lower Newtonian viscosity with less shear-thinning behavior.

Therefore, in our example below, we limit ourselves to the characterization of the apparent Newtonian viscosity of a polymer sample which can be estimated using the analytical correlation, Eq. (2.34). Once the apparent Newtonian viscosities are estimated from the MI data, we can use a power-law expression to correlate MWW with the viscosity.

Let us open the Excel spreadsheet, **Example 2.2 MI vs MWW.xlsx**. Columns B and C show the data of MI vs. MWW for LLDPE samples from Table 1 of [48]. See Figure 2.66. Based on Eq. (2.35), we can find column E from Column C, that is, $\mu = 7280 / \text{MI}$.

	A	B	C	D	E
1					
2					
3					
4					Step 1
5		Data (Bremner, Rudin, and Cook, 1990)			Calculate apparent Newtonian Viscosity
6		MWW (g/mol)	MI (g/10min)		Viscosity ($\mu\text{Pa}\cdot\text{s}$)
7		167000	0.3		24267
8		103000	0.6		12133
9		145000	1		7280
10		131000	0.8		9100
11		68000	1.2		6067
12		79000	4		1820
13		102000	2		3640
14		54000	20		364
15		48000	50		146
16		38000	100		73
17					

Figure 2.66 MI vs MWW for LDPE samples [48]

We then use Excel to develop a correlation between μ and MWW. See Figure 2.67. We note that this approach will work well for low MI materials where the flow through the melt indexer is primarily Newtonian.

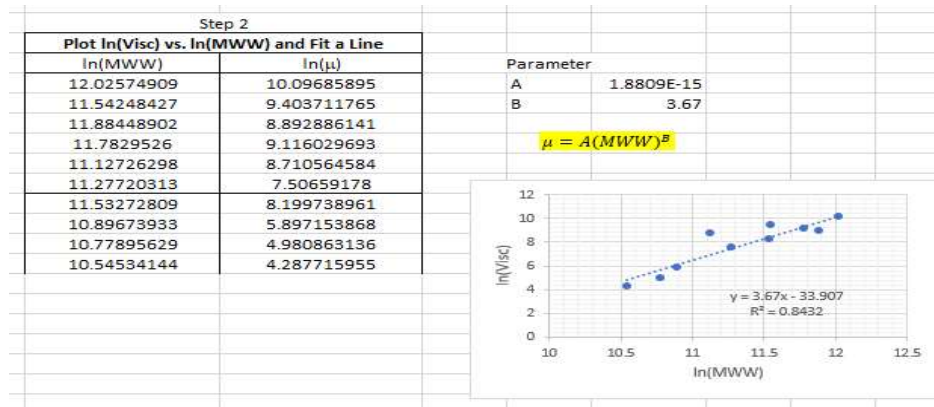


Figure 2.67 Developing a correlation between apparent Newtonian viscosity μ and MWW.

Finally, we note that we demonstrate how to implement the correlations for MI and polymer density, Eqs. (2.31) and (2.32), in steady-state polymer process simulation in Section 5.8.11 using FORTRAN in Aspen Polymers, and in dynamic polymer-grade changes using “Tasks” in Aspen Plus Dynamics in Section 7.6.3.

Conclusion

This chapter is published with Wiley publication in the book *Integrated Process Modeling, Advanced Control and Data Analytics for Optimizing Polyolefin Manufacturing* by Liu & Sharma. [55-68]

2.11 Bibliography

1. Walas, S. M. (1985). *Phase Equilibria in Chemical Engineering*, Butterworth, Stoneham, MA.
2. Bokis, C. P.; Orbey, H.; Chen, C. C. (1999). Properly Model Polymer Processes. *Chem. Eng. Prog.*, **95**, No. 4, 39, April.

3. Seavey, K. C.; Liu, Y. A. (2008). Step-Growth Polymerization Process Modeling and Product Design. Wiley, New York, pp. 87-92.
4. Chen, C. C. (1993). A Segment-Based Local Composition Model for Gibbs Energy of Polymer Solutions. Fluid Phase Equilib., **83**, 135.
5. Renon, H.; Prausnitz, J. M. (1968). Local Compositions in Thermodynamic Excess Functions for Liquid Mixtures. AIChE J., **14**, 135.
6. Flory, P. J. (1942). Thermodynamics of High Polymer Solutions. J. Chem. Phys., **10**, 51.
7. Flory, P. J. (1953). Principles of Polymer Chemistry. Cornell University Press, New York.
8. Huggins, M. L. (1942). Some Properties of Solutions of Long-Chain Compounds. J. Phys. Chem., **46**, 151.
9. Oishi, T.; Prausnitz, J. M. (1978). Estimation of Solvent Activity in Polymer Solutions Using a Group Contribution Method. Ind. Eng. Chem. Process Des. Dev., **17**, 333.
10. Fredenslund, A.; Jones, R. L.; Prausnitz, J. M. (1975). Group Contribution Estimation of Activity Coefficients in Nonideal Liquid Mixtures. AIChE J., **21**, 1086.
11. Fredenslund, A. (1977). Vapor-Liquid Equilibria Using UNIFAC: A Group-Contribution Method. Elsevier, New York.
12. Redlich, O.; Kwong, J. N. S. (1949). On the Thermodynamics of Solutions. V. An Equation of State. Fugacities of Gaseous Solutions. Chem. Rev., **44**, 233.
13. Van Krevelen, D. W.; Nijenhuis, K. te (2009). Properties of Polymers - Their Correlation with Chemical Structure; Their Numerical Estimation and Prediction from Additive Group Contributions. Fourth Edition, Elsevier, Amsterdam.
14. Painter, P. C.; Coleman, M. M. (1977). Fundamentals of Polymer Science: An Introductory Text. Second edition. Technomic Publishing Company, Inc., Lancaster, PA.
15. Lambert, S. M.; Song, Y.; Prausnitz, J. M. (2000). Equations of State for Polymer Systems. In J. V. Sengers, R. F. Kaye, C. J. Peters, and H. J. White (Eds.), Equations of State for Fluids and Fluid Mixtures. pp. 523-588. Elsevier, New York.
16. Wei, Y. S.; Sadus, R. J. (2000). Equations of State for Calculation of Fluid-Phase Equilibria. AIChE Journal, **46**, 169.
17. Sanchez, I. C.; Lacombe, R. H. (1976). An Elementary Molecular Theory of Classical Fluids. Pure Fluids. J. Phys. Chem., **80**, 2352.
18. Lacombe, R. H.; Sanchez, I. C. (1976). Statistical Thermodynamics of Fluid Mixtures., J. Phys. Chem. **80**, 2568.
19. Sanchez, I. C.; Lacombe, R. H. (1978). Statistical Thermodynamics of Polymer Solutions. Macromolecules, **11**, 1145.
20. McHugh, M. A.; Krukonis, V. J. (1994). Supercritical Fluid Extraction: Principles and Practice, 2nd edition. pp.99-134.

21. Gross, J.; Sadowski, G. (2001). Perturbed-Chain SAFT: An Equation of State Based on a Perturbation Theory for Chain Molecules. *Ind. Eng. Chem. Res.*, **40**, 1244.
22. Gross, J.; Sadowski, G. (2002). Modeling Polymer Systems Using of Perturbed-Chain SAFT Equation of State. *Ind. Eng. Chem. Res.*, **41**, 1084.
23. Gross, J.; Sadowski, G. (2002). Application of Perturbed-Chain SAFT Equation of State to Associating Systems. *Ind. Eng. Chem. Res.*, **41**, 5510.
24. Chapman, W. G., Gubbins, K. E.; Jackson, G.; Radosz, M. (1990). New Reference Equation of State for Associating Liquids. *Ind. Eng. Chem. Res.* **29**, 1709.
25. Huang, S. H.; Radosz, M. (1990). Equation of State for Small, Large, Polydisperse, and Associating Molecules. *Ind. Eng. Chem. Res.*, **29**, 2284.
26. Huang, S. H.; Radosz, M. (1991). Equation of State for Small, Large, Polydisperse, and Associating Molecules: Extension to Fluid Mixtures. *Ind. Eng. Chem. Res.* **30**, 1994.
27. Kang, J.; Zhu, L.; Xu, S.; Shao, Z.; Chen, X. (2018). Equation-Oriented Approach for Handling the Perturbed-chain SAFT Equation of State in Simulation and Optimization of Polymerization Process. *Ind. Eng. Chem. Res.*, **57**, 4697.
28. Khare, N.P.; Seavey, K. C.; Liu, Y.A.; Ramanathan, S.; Lingard, S.; Chen, C. C. (2002) Steady-State and Dynamic Modeling of Commercial Slurry High-Density Polyethylene (HDPE) Processes. *Ind. Eng. Chem. Res.* **41**, 5601.
29. Orbey, H., Bokis, C. P., Chen, C. C. (1998). Equation of State Modeling of Phase Equilibrium in the Low-Density Polyethylene Process: The Sanchez-Lacombe, Statistical Associating Fluid Theory, and Polymer-Soave-Redlich-Kwong Equations of State. *Ind. Eng. Chem.*, **37**, 4481.
30. Bokis, C. P., Ramanathan, S., Franjione, J., Buchelli, A., Call, M. L., Brown, A. L. (2002). Physical Properties, Reactor Modeling, and Polymerization Kinetics in the Low-Density Polyethylene Tubular Reactor Process. *Ind. Eng. Chem. Res.*, **41**, 1017.
31. Krallis, A.; Kanellopoulos, V. (2013). Application of Sanchez-Lacombe and Perturbed-Chain Statistical Fluid Theory Equation of State Models in Catalytic Olefins (Co)Polymerization Industrial Applications. *Ind. Eng. Chem. Res.*, **52**, 9060.
32. Hao, W.; Elbro, H. S.; Alessi, P. (1992). *Polymer Solution Data Collection. Chemistry Data Series*, XIV, Part 1, DECHME: Frankfurt, Germany.
33. Danner, R. P.; Hugh, M. S. (1993). *Handbook of Polymer Solution Thermodynamics*. Design Institute for Physical property Research, American Institute of Chemical Engineers, New York.
34. NIST (National Institute of Science and Technology), *NIST Chemistry Webbook, SRD69, Thermophysical Properties of Fluid Systems*, <https://webbook.nist.gov/chemistry/fluid/>, accessed May 15, 2021.
35. William, R. B.; Katz, D. L. (1954). Vapor-Liquid Equilibria in Binary Systems. Hydrogen with Ethylene, Ethane, Propylene, and Propane. *Ind. Eng. Chem.*, **46**, 2512.
36. Beaton, C. F.; Hewitt, G. F. (1989). *Physical Property Data for the Design Engineer*; Hemisphere Publishing Corp., New York.

37. Sychev, V. V.; Vasserman, A. A.; Golovsky, E. A.; Kozlov, A. D.; Spiridonov, G. A.; Tsymarny, V. A. (1987). *Thermodynamic Properties of Ethylene*; Hemisphere Publishing Corp., New York.
38. Olabisi, O.; Simha, R. (1975). "Pressure-Volume-Temperature Studies of Amorphous and Crystalline Polymers. I. Experimental. *Macromolecules*, **8**, 206.
39. Gaur, U.; Wunderlich, B. (1981). Heat Capacity and Other Thermodynamic Properties of Linear Macromolecules. II. Polyethylene. *J. Phys. Chem. Ref. Data*, **10**, 119.
40. Knapp, H.; Doring, R.; Oellrich, L.; Plocker, U.; Prausnitz, J. M. (1982). *Vapor-Liquid Equilibria for Mixtures of Low Boiling Substances; Chemistry Data Series: Vol VI, Part 1*; DECHEMA: Frankfurt, Germany.
41. Brandrup, J.; Immergut, E. H.; Grulke, E. A. (1999). *Polymer Handbook*, 4th edition, Wiley, New York.
42. Khare, N.P.; Lucas, B.; Seavey, K. C.; Liu, Y. A.; Sirohi, A.; Ramanathan, S.; Lingard, S.; Song, Y. ; Chen, C. C. (2004). Steady-State and Dynamic Modeling of Gas-Phase Polypropylene Processes Using Stirred-Bed Reactors. *Ind. Eng. Chem. Res.*, **43**, 884.
43. Griff, A. L. (2003). Melt Index Mysteries Unmasked. See: <https://griffex.com/wp-content/uploads/2020/09/Griff-meltindex.pdf>. Accessed May 16, 2021.
44. Sperati, C. A.; Franta, W. A.; Starkweather, H. W. (1953). The Molecular Structure of Polyethylene V. The effect of Chain Branching and Molecular Weight on Physical Properties., *J. Amer. Chem. Soc.*, **75**, 6127.
45. Sinclair, K. B. (1983). "Characteristics of Linear LDPE and Description of the UCC Has Phase Process", Process Economics Report, SRI International, Menlo Park, CA.
46. Seavey, K. C.; Khare, N. P.; Liu, Y. A.; Bremner, T.; Chen, C. C. (2003). Quantifying Relationships among the Molecular Weight Distribution, Non-Newtonian Shear Viscosity and Melt Index for Linear Polymers. *Ind. Eng. Chem. Res.*, **42**, 5354.
47. Mattos Neto, A. G.; Freitas, M. F.; Nele, M.; Pinto, J. C. (2005). Modeling Ethylene/1-Butene Copolymerization in Industrial Slurry Reactors. *Ind. Eng. Chem. Res.*, **44**, 2697.
48. Meng, W.; Li, J.; Chen, B.; Li, H. (2013). Modeling and Simulation of Ethylene Polymerization in Industrial Slurry Reactor Series. *Chin. J. Chem. Eng.*, **21**, 850.
49. Aspen Technology, Inc. (2020). Top Questions about Aspen Polymer Process Modeling in Aspen Plus. AspenTech FAQ. <https://www.aspentech.com/en/resources/faq-documents/top-questions-about-polymer-process-modeling-in-aspen-plus>, accessed June 4, 2021.
50. Bremner, T.; Rudin, A.; Cook, D. G. (1990). Melt Flow Index Values and Molecular Weight Distributions of Commercial Thermoplastics. *J. Appl. Polym. Sci.* **41**, 1617.
51. Rohlfig, D. C.; Janzen, J. (1997). What is Happening in the Melt-Flow Plastometer: The Role of Elongational Viscosity. *Ann. Tech. Conf.-Soc. Plast. Eng.* p. 1010.

52. Liu, Y. A., & Sharma, N. (2023). *Integrated Process Modeling, Advanced Control and Data Analytics for Optimizing Polyolefin Manufacturing*. Wiley-VCH GmbH (<https://doi.org/10.1002/9783527843831>)
53. Sharma, N., & Liu, Y. A. (2019). 110th anniversary: an effective methodology for kinetic parameter estimation for modeling commercial polyolefin processes from plant data using efficient simulation software tools. *Industrial & Engineering Chemistry Research*, 58(31), 14209-14226. <https://doi.org/10.1021/acs.iecr.9b02277>
54. Sharma, N., & Liu, Y. A. (2022). A hybrid science-guided machine learning approach for modeling chemical processes: A review. *AIChE Journal*, 68(5), e17609. <https://doi.org/10.1002/aic.17609>
55. Liu, Y. A., & Sharma, N. (2023). Introduction to Integrated Process Modeling, Advanced Control, and Data Analytics in Optimizing Polyolefin Manufacturing. In *Integrated Process Modeling, Advanced Control and Data Analytics for Optimizing Polyolefin Manufacturing* (Chapter 1, pp. 1-40). Wiley-VCH GmbH. <https://doi.org/10.1002/9783527843831.ch1>
56. Liu, Y. A., & Sharma, N. (2023). Selection of Property Methods and Estimation of Physical Properties for Polymer Process Modeling. In *Integrated Process Modeling, Advanced Control and Data Analytics for Optimizing Polyolefin Manufacturing* (Chapter 2, pp. 41-86). Wiley-VCH GmbH. <https://doi.org/10.1002/9783527843831.ch2>
57. Liu, Y. A., & Sharma, N. (2023). Reactor Modeling, Convergence Tips, and Data-Fit Tool. In *Integrated Process Modeling, Advanced Control and Data Analytics for Optimizing Polyolefin Manufacturing* (Chapter 3, pp. 87-114). Wiley-VCH GmbH. <https://doi.org/10.1002/9783527843831.ch3>
58. Liu, Y. A., & Sharma, N. (2023). Free Radical Polymerizations: LDPE and EVA. In *Integrated Process Modeling, Advanced Control and Data Analytics for Optimizing Polyolefin Manufacturing* (Chapter 4, pp. 115-162). Wiley-VCH GmbH. <https://doi.org/10.1002/9783527843831.ch4>
59. Liu, Y. A., & Sharma, N. (2023). Ziegler–Natta Polymerization: HDPE , PP , LLDPE, and EPDM. In *Integrated Process Modeling, Advanced Control and Data Analytics for Optimizing Polyolefin Manufacturing*. (Chapter 5, pp. 163-265). Wiley-VCH GmbH. <https://doi.org/10.1002/9783527843831.ch5>
60. Liu, Y. A., & Sharma, N. (2023). Free Radical and Ionic Polymerizations: PS and SBS Rubber. In *Integrated Process Modeling, Advanced Control and Data Analytics for Optimizing Polyolefin Manufacturing*. (Chapter 6, pp. 267-319). Wiley-VCH GmbH. <https://doi.org/10.1002/9783527843831.ch6>
61. Liu, Y. A., & Sharma, N. (2023). Improved Polymer Process Operability and Control Through Steady-State and Dynamic Simulation Models. In *Integrated Process Modeling, Advanced Control and Data Analytics for Optimizing Polyolefin Manufacturing*. (Chapter 7, pp. 321-379). Wiley-VCH GmbH. <https://doi.org/10.1002/9783527843831.ch7>
62. Liu, Y. A., & Sharma, N. (2023). Model-Predictive Control of Polyolefin Processes. In *Integrated Process Modeling, Advanced Control and Data Analytics for Optimizing Polyolefin Manufacturing*. (Chapter 8, pp. 381-476). Wiley-VCH GmbH. <https://doi.org/10.1002/9783527843831.ch8>

63. Liu, Y. A., & Sharma, N. .2023. Application of Multivariate Statistics to Optimizing Polyolefin Manufacturing. In *Integrated Process Modeling, Advanced Control and Data Analytics for Optimizing Polyolefin Manufacturing* (Chapter 9, pp. 477-531). Wiley-VCH GmbH.
<https://doi.org/10.1002/9783527843831.ch9>
64. Liu, Y. A., & Sharma, N. (2023). Applications of Machine Learning to Optimizing Polyolefin Manufacturing. In *Integrated Process Modeling, Advanced Control and Data Analytics for Optimizing Polyolefin Manufacturing*. (Chapter 10, pp. 553-650). Wiley-VCH GmbH.
<https://doi.org/10.1002/9783527843831.ch10>.
65. Liu, Y. A., & Sharma, N. (2023). A Hybrid Science-Guided Machine Learning Approach for Modeling Chemical and Polymer Processes. In *Integrated Process Modeling, Advanced Control and Data Analytics for Optimizing Polyolefin Manufacturing*. (Chapter 11, pp. 651-698). Wiley-VCH GmbH.
<https://doi.org/10.1002/9783527843831.ch11>
66. Sharma, N. and Liu, Y., 2019, November. Polyolefin Process Modeling and Monitoring. In *2019 AIChE Annual Meeting*. AIChE.
67. Sharma, N. and Liu, Y., 2020, November. Polyolefin Process Improvement Using Machine Learning. In *2020 Virtual AIChE Annual Meeting*. AIChE
68. Sharma, N., 2022, November. Polyolefin Property Estimation using Process Modeling and Machine Learning in Industry. In *2022 AIChE Annual Meeting*. AIChE.
-